Environmental Health Perspectives
Vol. 55, pp. 369-390, 1984

Deposition and Clearance of Inhaled Particles

by Bruce O. Stuart*

Theoretical models of respiratory tract deposition of inhaled particles are compared to experimental studies of deposition patterns in humans and animals, as governed principally by particle size, density, respiratory rate and flow parameters. Various models of inhaled particle deposition make use of approximations of the respiratory tract to predict fractional deposition caused by fundamental physical processes of particle impaction, sedimentation, and diffusion. These models for both total deposition and regional (nasopharyngeal, tracheobronchial, and pulmonary) deposition are compared with early and recent experimental studies. Reasonable correlation has been obtained between theoretical and experimental studies, but the behavior in the respiratory tract of very fine (< 0.1 μm) particles requires further investigation. Properties of particle shape, charge and hygroscopicity as well as the degree of respiratory tract pathology also influence deposition patterns; definitive experimental work is needed in these areas. The influence upon deposition patterns of dynamic alterations in inspiratory flow profiles caused by a variety of breathing patterns also requires further study, and the use of differing ventilation techniques with selected inhaled particle sizes holds promise in diagnosis of respiratory tract diseases. Mechanisms of conducting airway and alveolar clearance processes involving the pulmonary macrophage, mucociliary clearance, dissolution, transport to systemic circulation, and translocation via regional lymphatic vessels are discussed.

Introduction

Human populations have often encountered inhalation exposures to clouds of airborne particles caused by natural phenomena, including forest fires and volcanic eruptions. These exposures may be hazardous or fatal, depending on air concentration, particle size, and composition of suspended materials, as reported in the recent Mt. St. Helen's eruption (*1*). However, for thousands of years man has also been creating his own hazardous aerosols while mining or roasting metal ores to make tools and weapons, as well as in the extraction and use of fossil fuels. In sixteenth century Europe, a corrosive cadmia (arsenical cobalt) was described that destroyed miners' lungs (*2*). Drinker and Hatch (*3*) have shown that the occurrence of chronic respiratory diseases increased greatly as a consequence of the continuing search for metal ores, particularly during the last 300 years. Ludwig and Lorenser (*4*) have described a high incidence of lethal "Bergkrankheit" that existed for centuries among miners of Saxony and Joachimsthal, caused principally by inhaled metal ore dusts and airborne radioactivity attached to dust particles.

In 1916, Watkins-Pitchford and Moir (*5*) recognized the importance of inhaled particle size, finding 80% of the particles in silicotic human lungs to be < 2 μm in diameter. Hatch and Gross (*6*) report that inhalation exposure to aerosols of fine (< 0.6 μm) zinc oxide particles can cause "metal-fume fever," but exposure to similar air concentrations of zinc oxide derived from coarse bulk material is not toxic. Measurement of the concentration of airborne contaminant particles and the total inhaled air volume was found to be insufficient to predict the pathological effects of inhalation exposure, or to evaluate the relative hazard of exposure to a particular aerosol, whether dust or mist. The size distribution and density of aerosol particles determines their depth of penetration as well as their fractional deposition within the respiratory tract, locating their critical sites of action and their related clearance or translocation mechanisms. The physiological parameters that affect deposition of aerosols need further definition. These should include further studies of effects upon dynamic respiratory flow profiles, air movement and airway constriction caused by exposure to reactive agents (*7*), and changes caused by impairment of ventilation resulting from chronic respiratory disease (*8,9*). Here the term, aerosol, refers to a system of solid or liquid particles of sufficiently small diameter to maintain stability as a suspension in air, as defined by Green and Lane (*10*).

In order to describe the risk from inhaled hazardous aerosols, one must know how much is deposited in a specified region of the respiratory tract and how much remains after physiological clearance from that region. The remaining material (i.e., the retained material) is the effective dose of air contaminant that can produce acute or chronic pulmonary disease. Predictive models and experimental evaluation of the deposition of mate-

*Toxic Hazards Division, Air Force Aerospace Medical Research Laboratory, Area B, Wright Patterson Air Force Base, OH 45433

rial within the entire respiratory tract (total deposition) are necessary in the case of soluble aerosols, because these contaminants can reach the bloodstream or lymphatic channels from several regions of the respiratory tract. Predictive models and experimental measurements of the regional deposition of insoluble aerosols are important, particularly for those fractions of aerosols that are deposited in the distal regions of the respiratory tract located beyond the ciliated epithelium, because these materials will clear only gradually. These fractions may remain as persistent reservoirs of incorporated contaminants, able to cause chronic pulmonary or systemic disease.

Deposition is the crucial first step in determining subsequent clearance processes. As discussed by the Task Group on Lung Dynamics (*11*), the respiratory tract can be described in terms of three compartments based upon the clearance mechanisms associated with each region. Inhaled particles deposited in the posterior nares will be caught up in mucus and conveyed by mucociliary action through the nasopharynx, and into the gastrointestinal tract (*12*). Airborne particles reaching the larynx and passing through successive generations of conducting airways to the terminal bronchioles will also be deposited upon mucus that is propelled upwards by underlying cilia for clearance to the gastrointestinal tract. Inhaled insoluble particles that are deposited below the ciliated epithelium, i.e., on the surfaces of the respiratory bronchioles, alveolar ducts, alveolar sacs and alveoli, will be cleared more slowly to the gastrointestinal tract, or will remain with only gradual dissolution or removal following phagocytosis by pulmonary macrophages.

The Respiratory Tract

Inhaled aerosols may first encounter coarse hairs within the anterior nares that will impede or intercept the larger particles, and will promote their impaction upon the walls of the airways shown in Figure 1. The aerosol is then drawn through the posterior nares, becoming warmed and humified as it passes over flattened projections (conchae). The aerosol particles next enter the nasopharyngeal region, characterized by stratified squamous epithelium, which extends from the oral pharynx to the larynx.

Aerosol flow passes through the trachea and divides into the right and left bronchi; these separate into secondary lobar branches and subsegmental branches, finally dividing into smaller quaternary branches numbering more than 800 (*13*). This branching extends into smaller conducting airways where mucus-producing goblet cells and secretory glands gradually disappear, and the epithelial lining becomes nonciliated at the level of the terminal bronchioles. Terminal bronchioles separate into respiratory bronchioles that are nonciliated and number nearly 150,000 (*14*). Respiratory bronchioles divide into alveolar ducts that are almost entirely lined with alveoli; there are about 26 million of these

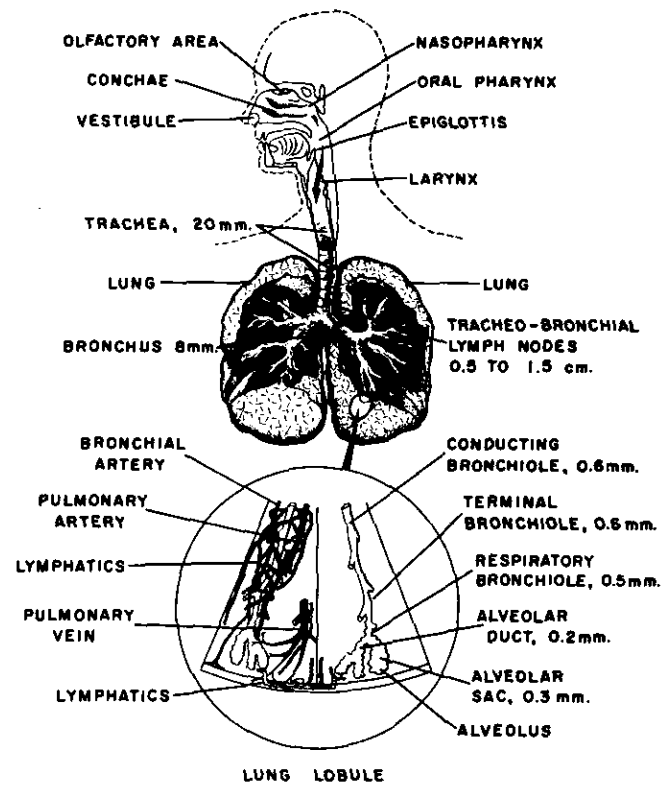

FIGURE 1. Anatomy of the respiratory tract. Courtesy of the National Academy of Sciences, NAS-NRC Publication 848.

ducts (*15*), giving rise to 50 to 100 million alveolar sacs (*16*). These sacs provide 30 to 100 m^2 of gas exchange surface in adult human lungs, depending upon individual body size and exercise level (*8*).

Alveolar walls are composed of reticular and elastic fibers forming a network that supports fine pulmonary capillaries. Lymphatic channels are present throughout the pleura and septa, draining into regional lymph nodes. These channels may constitute an important avenue of pulmonary clearance of insoluble deposited particles (*17*). Hilar lymph nodes may become secondary reservoirs of deposited material, causing prolonged release of hazardous inhaled materials to the systemic circulation (*18*).

In the course of normal respiration, rates of air flow entering the respiratory tract may range from zero to a maximum of 60 to 120 L/min, depending upon the amount of work being performed (*8,19*). During both inspiration and expiration, deposition processes that follow physical laws will take place. The three principal mechanisms of deposition are inertial impaction, sedimentation, and diffusion. Particle deposition as a function of electrical charge (image diffusion) is believed to be of secondary importance except where very highly charged particles are generated (*11*). Deposition mechanisms are greatly influenced by changes in air flow and by the differences in residence times at each level of the respiratory tract that occur during each cycle of complete respiration (*20*). At a ventilation rate of 200

mL/sec, linear air flow rates will range from 180 cm/sec in the main bronchi to only 0.025 cm/sec in alveolar ducts (*19*).

Mechanisms of Deposition

Inertial impaction of inhaled particles is the principal mechanism of large particle deposition in the upper regions of the respiratory tract, acting on particles ranging from 2 to 3 μm to greater than 20 μm in diameter. The inertia of a large airborne particle will tend to maintain its initial path when the supporting airstream is suddenly deflected by nasal turbinates or branching of airways. The probability I of inertial deposition is proportional to the terminal settling velocity V_t of the entrained particle, times the velocity of the airstream V_a and inversely proportional to the radius R of the airway:

$$I \propto (V_t V_a \sin \theta)/gR$$

where g is the gravitational constant. The larger the particle, the greater the settling velocity. At increasing air velocity, greater bend angles θ and smaller airway radii, there will be greater probability of deposition by inertial impaction (*21*).

Sedimentation, or settling under the force of gravity, is also an important mechanism for particle deposition in the respiratory tract. A particle falling in air accelerates to a terminal settling velocity V_t at which the force of gravity is balanced by the resistance of the air:

$$V_t = (\rho - \sigma)gd^2/18\gamma$$

where γ is the viscosity of air, and ρ and σ are the densities of the particle and of air, respectively. As the particle diameter d becomes very small, i.e., of the same order as the mean free path of air molecules (λ), air resistance decreases, and a correction factor (*22*) must be applied:

$$V_t(\text{actual}) = V_t(\text{calculated}) [1 + (2A\lambda/d)]$$

where $A = 1.26 + 0.4^{-1.1d/2\lambda}$. This terminal settling velocity may be approximated as $2.9 \times 10^5 \times (\rho d^2)$ cm/sec (*23*).

The foregoing discussion illustrates the governing parameters of particle density and size in the principal mechanisms of deposition. Deposition models are frequently based upon a technique of normalizing using the "aerodynamic equivalent diameter," defined as the diameter of a unit density sphere that has the same terminal settling velocity (V_t) as the given particle. In the lung, inhaled particles within an airway will fall a distance $V_t t$, where t is the time of travel. If the airway containing the particle is at a given angle ϕ with the horizontal, then the ratio of the distance of fall to maximum distance for deposition becomes $V_t t \cos \phi/2R$, where R is airway radius. Landahl (*21*) stated the probability of S deposition by sedimentation as:

$$S = 1 - \exp \{(-0.8V_t\, t \cos \phi)/R\}$$

Sedimentation is one of the primary mechanisms of deposition of inhaled particles having diameters ranging from 0.1 μm to 50 μm (*24*).

Deposition by diffusion or Brownian motion in the respiratory tract predominates for very small particle sizes, i.e., < 0.2 μm. These particles are displaced by the random thermal motion of the gas molecules of air. This displacement Λ is inversely proportional to the viscosity of the air γ and to the diameter of the particle d, and is directly proportional to the residence time t of the particle in a given air space:

$$\Lambda = [(RT/N)\ (Ct/3\pi\gamma d)]^{1/2}$$

where R, T and N are the ideal gas constant, the absolute temperature, and Avogadro's number, respectively, and C is Cunningham's correction (*22*). Thus the probability of deposition by diffusion D will increase as the displacement motion is increased relative to the size of the confining space (*21*):

$$D = 1 - \exp \{-0.58\Lambda/R\}$$

This mechanism of deposition increases with decreasing particle size, whereas deposition by sedimentation decreases with decreasing particle size, and as a result there occurs a minimum deposition at which the displacement velocity due to terminal settling is low and the displacement velocity due to diffusion is also low. This occurs with aerodynamic particle diameters of roughly 0.2 to 0.5 μm (*6*), as illustrated in Table 1.

These physical mechanisms describe the deposition of inhaled particles, but deposition fractions are also highly dependent upon the individual dimensions of air passages, the rate of air flow into each airway genera-

Table 1. Root-mean-square Brownian displacement per second and terminal velocity in air.[a]

Diameter, μm[b]	Brownian displacement, λ, cm	Terminal velocity V_t cm/sec
Terminal velocity		
40	1.4×10^{-4}	4.8
20	1.4×10^{-4}	1.2
10	2.0×10^{-4}	2.9×10^{-1}
4	3.5×10^{-4}	5.0×10^{-2}
2	5.0×10^{-4}	1.3×10^{-2}
1	7.4×10^{-4}	3.5×10^{-3}
0.6	1.0×10^{-3}	1.4×10^{-3}
0.4	1.3×10^{-3}	6.8×10^{-4}
0.2	2.1×10^{-3}	2.3×10^{-4}
0.1	3.6×10^{-3}	8.6×10^{-5}
0.06	5.7×10^{-3}	4.7×10^{-5}
0.04	8.1×10^{-3}	2.9×10^{-5}

[a] From Hatch and Gross (*6*)
[b] Unit density spheres, 760 mm Hg and 20°C.

tion, and the residence time of the particle in each airway. In 1980 Heyder, et al. (*25*) demonstrated that sedimentation and impaction are competing mechanisms in the respiratory tract, with sedimentation primarily a function of mean residence time of inhaled particles, and with impaction depending upon their mean flow rate within an airway. Sedimentation was suggested as the major mechanism of deposition for particles > 1 μm at increased residence times and decreased flow rates (which also promotes deposition by diffusion of very small particles), while impaction was major mechanism of deposition at decreased particle residence times and increased flow rates. At fixed respiratory frequency and flow rate, impaction affects the largest particles and occurs in upper regions of the respiratory tract where airflows are high. Deposition by sedimentation will predominate at small generations of bronchi or bronchioles, and in the parenchymal lung, having a major influence on deposition of particles down to sizes of 0.5 to 1 μm (aerodynamic diameter). Diffusion is independent of density and affects the smallest particles, i.e., 0.5 μm to < 0.002 μm (*24*). This occurs principally in the small airway and gas exchange regions of the lung, but extremely small particles such as condensation nuclei may deposit in the nasopharynx very shortly after entrance into the respiratory tract, as a result of their high Brownian displacement (*10*).

Increased deposition in successively distal regions in the respiratory tract may also occur upon the rapid increase in diameter of hygroscopic particles during passage through the high humidity of the respiratory tract (*11*). Wilson and LaMer (*26*) found that pulmonary deposition of glycerol particles labeled with radioactive ^{24}Na agreed with predicted deposition values when the particle diameters were corrected for growth in the 99.5% relative humidity of the respiratory tract. Dautrebande and Walkenhorst (*27*) found reasonable agreement with predicted deposition fractions of inhaled sodium chloride particles when correction was made particle size increase in high humidity. Generally, the effect of hygroscopicity on deposition will be less for particles composed of materials having larger densities and higher molecular weight. As discussed by Raabe (*28*), particles of ammonia sulfate or sulfite, as well as hygroscopic H_2SO_4, will grow in the respiratory tract when inhaled, causing increased loss by impaction in upper airways; a 1 μm particle may grow by water absorption to 3 μm in the nasopharynx, causing a 2-fold increase in nasal and tracheobronchial deposition. Sinclair (*29*) has shown that hygroscopic growth of atmospheric particles < 2 μm may significantly increase their deposition.

A nonspherical shape (fibers or ellipsoids) may greatly affect deposition. Abnormalities arise in the case of fibrous materials such as asbestos; i.e., fibers greater than 50 μm in length have been found within the alveoli of experimental animals (*30*). Beeckmans (*31*) has concluded that although there may be little change in the proportion of inhaled particles deposited in the lower respiratory tract as a function of shape, the mass of the individual particles in the maximum deposition range tends to increase as particles become more elongated. Fibers with length-to-diameter ratio of greater than 10 have been shown by Timbrell and Skidmore (*30*) to have an aerodynamic diameter roughly 3-fold greater than the fiber diameter. Lippmann (*32*) suggests that fibers > 100 μm in length with a fiber diameter of 1 μm would have low probability of deposition by impaction, but much higher probability of interception, especially for curved fibers, e.g., chrysolite asbestos.

Electrical charges on particles in aged aerosols will approach Boltzman equilibrium and will not greatly influence deposition fractions of such aerosols. However, Mercer (*33*) indicates that freshly generated particles may be highly charged, and Melandri et al. (*34*) have found that respiratory tract deposition can increase by 30% for highly charged particles, probably due to image charging at the walls of conducting airways. Particles generated by grinding or combustion are electrically charged, but the net charge of these aerosols, if aged, is usually negligible (*11*). Although there may be increased aggregation of small individually charged particles, there is probably small effect upon total deposition in the respiratory tract. However, very small charged particles have higher mobilities and may show greater deposition in the nasopharynx than do noncharged particles. Vincent et al. (*35*) recently found that static electrification of amosite asbestos (260 electrons/fiber) increased alveolar deposition (slowest clearing region) by 40% in rat lungs.

Inhaled Particle Deposition in the Respiratory Tract: Predictive Models and Experimental Studies

Deposition in the Total Lung

The first comprehensive theoretical treatment of total respiratory tract deposition was developed by Findeisen (*36*) in 1935, based on a model consisting of the trachea, four generations of bronchi, two generations of bronchioles, alveolar ducts and alveolar sacs; the results are shown in Figure 2. Landahl (*21,37*) in 1950 described a model including mouth and pharynx with two orders of alveolar ducts; using 3/8 of the respiratory cycle for inspiration and 3/8 for expiration (curves *2,3,4* of Fig. 2). In 1949 Sinclair and LaMer (*38*) developed a generator that produced monodispersed aerosols, i.e., aerosols of a single particle size. These were used in tests by Landahl et al. (*37*) in which fractions of exhaled air were collected and analyzed (curve *7*). Altschuler et al. (*39*) examined deposition of monodispersed aerosols of density 1.3 g/cm^3, finding a deposition minimum at 0.4 μm, as predicted by their model, and that slow, deep breathing increased deposition. In 1965 Beeckman (*40*) examined Landahl's model using computer simulations

to determine the effect of recycled nondeposited aerosols and interpulmonary gas mixing (curve *5*); this model also predicted decreased total deposition as tidal volume was decreased. Dennis (*41*) used stearic acid particles to study total respiratory tract deposition; fractions increased as respiration rates were lowered below 15 cycles/min (curve *10*). Curve *11* presents studies of coal dust deposition made by Walkenhorst and Dautrebande (*42*). Davies (*43*) derived formulae based on continuity between suspended and deposited aerosol fractions for prediction of deposition fractions (curve *12*).

In 1959 the International Commission on Radiological Protection (ICRP) developed a working model to describe roughly the deposition of inhaled dust (*44*). They assumed 75% of the mass of all inhaled dust was deposited, with 25% exhaled. Two-thirds was deposited in the "upper respiratory" tract (i.e., from the exterior nares to the larynx), and one-third in the "lower respiratory" tract, with differing clearance patterns, for soluble or insoluble dusts. This extremely simple model provided the initial design of safety procedures involving airborne radioactive particles, but ignored the effects of particle size and density on deposition fractions, and did not describe deposition sites that could be correlated with subsequent clearance patterns.

The Task Group on Lung Dynamics was established in 1966 by the International Committee on Radiological Protection to develop a deposition model for inhaled particles using data based on a three-compartment model of the respiratory tract (*11*). The "nasopharynx"

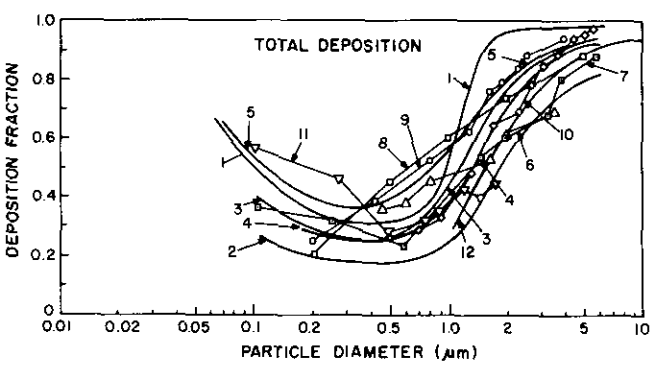

FIGURE 2. Predictive models and experimental values for total deposition of inhaled particles: (1) predictive, Findeisen (36), 200 mL/sec, 14 respirations/min; (2) predictive, Landahl (*21*), 300 mL/sec, 5 respirations/min, tidal volume 450 mL; (3) predictive, Landahl (*21*), 300 mL/sec, 7.5 respirations/min, tidal volume 900 mL; (4) predictive, Landahl (*21*), 1000 mL/sec, 15 respirations/min, tidal volume 1500 mL; (5) theoretical, Beeckmans (*40*), 5 respirations/min, tidal volume 1350 mL; (6) experimental, Wilson and LaMer (*26*), 5.5 respirations/min; (7) experimental, Landahl et al. (*37*), 7.5 respirations/min, tidal volume 900 mL; (8) experimental, Gessner et al. (*93*), 15 respirations/min, tidal volume 700 mL; (9) experimental, Van Wijk and Patterson (*46*), 19 respirations/min, tidal volume 700 mL; (10) experimental, Dennis (*41*), 13.3 respirations/min, tidal volume 720 mL; (11) experimental, Dautrebande and Walkenhorst (*27*), 10 respirations/min, tidal volume 990 mL; (12) experimental, Davies (*43*), 15 respirations/min, tidal volume 600 mL.

consisted of the anterior and posterior nares, plus the oralpharynx; the "tracheobronchial" region extended from the larynx to the terminal bronchioles, composed of airways having ciliated epithelium; the "pulmonary" region included respiratory bronchioles, alveolar ducts, alveolar sacs and alveoli; i.e., the gas exchange region of the lung. It was based on the real world conditions that air contaminants are usually inhaled as dispersed aerosols that can be frequently described by log normal distributions of particle diameters. Deposition fractions were described in terms of the aerosol particle size distribution, i.e., the mass median aerodynamic diameter (MMAD). Values for deposition by diffusion were obtained by the use of the Gormley-Kennedy equations for laminar flow in tubes (*45*). Reasonable agreement was obtained between predictive deposition curves for monodispersed particles and the experimental results of Van Wyck and Patterson (*46*), Dautrebande and Walkenhorst (*27*) and Dennis (*41*). Little variation was found for aerosols of widely different degrees of dispersity of particle sizes within an aerosol; i.e., different geometric standard deviations. Similar curves were found for tidal volumes of 750, 1450 and 2150 mL, suggesting that although an individual's minute volume (tidal volume times respiration rate) controls the total amount of dust inhaled and deposited, it has relatively little affect on deposition fractions.

Following these earlier studies, several carefully executed studies were conducted to measure the deposition in humans of monodispersed insoluble aerosols, assessed as a function of different breathing parameters. These experiments were performed under strictly controlled conditions of uniform particle size generation and characterization, and involved trained human volunteers. They include the work of Lippmann and Albert (*47*), Giacomelli-Maltoni et al. (*48*), Foord et al. (*49*), Swift et al. (*50*), Chan and Lippmann (*51*), and Heyder et al. (*25,52*). George and Breslin (*53*) and Holleman et al. (*54*) have provided data on the measured deposition of inhaled attached radon daughters. Hounam (*55*), Hounam et al. (*56*) and Fry and Black (*57*) have provided further information on nasopharyngeal deposition. Figures 3 and 4 show the results of these more recent studies under carefully controlled conditions in comparison with the derived curves of the Task Group on Lung Dynamics (hereafter referred to as the TGLD) for total deposition in the respiratory tract following nasal breathing and mouth breathing, respectively (*11*). Since particle behavior is essentially independent of density below 0.5 μm, the actual physical or linear diameter is indicated.

Figure 3 shows the experimental data obtained by Giocomelli-Maltoni et al. (*48*) using monodispersed aerosols of carnuba wax generated by condensation of the vapor to form solid hydrophobic particles. These studies employed healthy adults, using light scattering techniques for measurement of particle concentrations in the inhaled and exhaled air. Heyder et al. (*58*) conducted experiments involving five normal subjects,

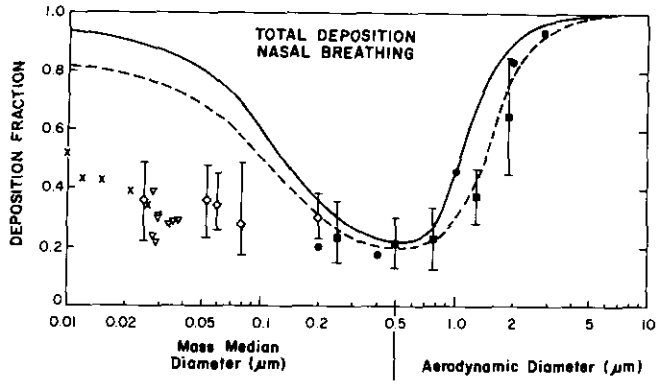

FIGURE 3. Total respiratory tract deposition of inhaled particles during nasal breathing: (■) Giacomelli-Maltone et al. (*48*), tidal volume (TV), 1500 mL, 12 respirations per minute (RPM), (◇) George and Breslin (*53*), TV 550–760 mL, 14 RPM; (●) Heyder et al. (*58*) TV 1000 mL, 15 RPM, (×) Holleman et al. (*54*), TV 1200 mL, 15 RPM; (——) Task Group on Lung Dynamics (*11*), TV 1450 mL, 15 RPM, (--) TV 750 mL, 15 RPM, (▽) Swift et al. (*50*), TV 1150 mL, 18 RPM.

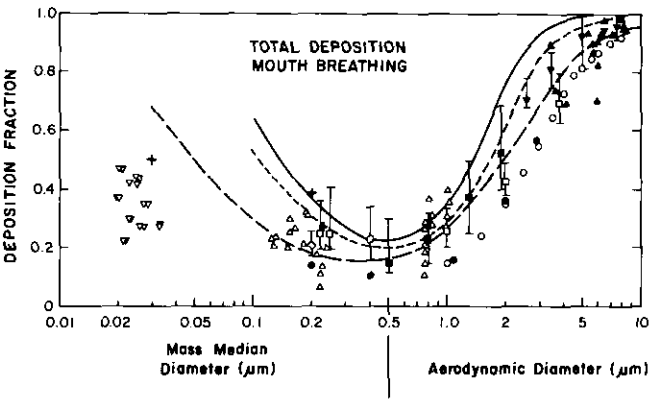

FIGURE 4. Total respiratory tract deposition of inhaled particles during mouth breathing: (■) Giacomelli-Maltoni et al. (*48*), TV 1000 mL, 12 RPM; (●) Heyder et al. (*58*), TV 1000 mL, 15 RPM; (Δ) Chan and Lippmann (*51*), TV 1000 mL, 14 RPM; (○) Heyder et al. (*25*), TV 1000 mL, 15 RPM; (▲) Lippmann and Albert (*47*), TV 1400 mL, 14 RPM; (▼) Foord et al. (*49*), TV 1000 mL, 15 RPM; (+) Hursh and Mercer (157), TV ~ 1500 mL, 15 RPM; (▽) Swift et al. (*50*), TV 500 mL, 15 RPM; (——) Task Group on Lung Dynamics (*11*), TV 1450 mL, 15 RPM; (--) TV 750 mL, 15 RPM; (×) Yu et al. (*62*), TV 1000 mL, 15 RPM; bars represent three times the standard deviation (3SD).

studying total deposition during nose and mouth breathing using monodispersed di-2-ethyl hexyl sebacate droplets with diameters of 0.1 to 3.2 μm. Both predictive curves and experimental data indicate 100% deposition above 5 μm. The size for minimum deposition occurred between 0.1 and 0.8 μm.

Although most recent studies have centered upon particles ranging from 0.1 to 10 μm, it is possible that very small particles (< 0.01 to 0.1 μm) having very high diffusion rates may deliver extremely high radiological doses to localized regions of the respiratory tract, if they are high in specific radioactivity. The short-lived alpha-emitting daughters of radon are a case in point (*59,60*). Depending upon whether these radioactive atoms are free (unattached) or are attached to atmospheric dust particles, a difference in delivered dose of greater than 10-fold is possible (*59*). Figure 3 includes data obtained in human volunteers by Holleman et al. (*54*), who studied the deposition of radon daughters in the uranium mines of the Colorado plateau using diffusion tube measurements to characterize particle size; in this case the diameters are activity median diameters. George and Breslin (*53*) conducted laboratory and uranium mine experiments using a diffusion battery for particle size measurements and found that total deposition in humans of inhaled radon daughters ranged from 23% to 45%. Deposition increased with decreasing particle size and with increasing tidal volume, both characteristic of very fine particles depositing by diffusion in the respiratory tract. Particle size for attached radon daughters was found to vary greatly with location in the mine, a finding substantiated by Palmer, et al. (*61*) in uranium mines on the Colorado Plateau. The critical interaction between attachment of these radionuclides and subsequent deposition was shown by George and Breslin (*53*); total depositions during nasal breathing were 2% and 62%, respectively, for attached and unattached radon daughters.

The two continuous curves predicted by the TGLD (*11*) at 15 respirations per minute with tidal volume of 1450 and 750 mL show reasonable agreement with the experimental data obtained by Giacomelli-Maltoni et al. (*48*) and Heyder et al. (*58*) for particle sizes down to 0.2 μm. However, deposition fractions are markedly different from the observed experimental results for particle sizes ranging from 0.2 to 0.01 μm, which are the critical sizes for deposition of attached and unattached radon daughters. For these sizes total respiratory tract deposition is overestimated by at least a factor of 2, with a corresponding error in absorbed radiological or chemical dose to sensitive epithelial cells.

The continuous curve developed by Yu et al. (*62*) in 1978 was based upon a two-compartment theory for aerosol deposition, reflecting recent experimental results (*63*). Lippmann and Albert (*47*) in 1969 reported results from precise measurements using human volunteers inhaling insoluble Fe_2O_3 aerosols labeled with ^{198}Au or ^{99m}Tc, using external measurements of gamma photons emitted from different regions of the respiratory tract; the amount of material that disappeared from the region of the chest during the first 24 hr was used as a measurement of tracheobronchial deposition (*47*). Foord et al. (*49*) in 1978 studied total alveolar deposition in 16 subjects using polystyrene particles of 2.5 to 7.5 μm diameter labeled with ^{99m}Tc. Deposition fractions were obtained by measuring the difference between inhaled and exhaled aerosol radioactivities, and amounts of deposited radioactivity that were subsequently excreted. Heyder et al. (*58*) in 1975, Heyder

and Davies (*52*) and Heyder et al. (*25*) in 1980 used two methods of determining total deposition data. The first procedure (digital method) measured directly the quantity of inspired and expired particles of Fe_2O_3 labeled with ^{198}Au by external monitoring. The second method involved continuous monitoring of the particle number concentration and volume flow rate (analog method). In 1975 Heyder et al. (*58*) reported total deposition data from five subjects for nose and mouth breathing using monodispersed aerosols of di-2-ethylhexyl sebacate droplets with diameters ranging from 0.1 to 3.2 μm, under well-defined breathing patterns. The particle size for minimum deposition was found to be a function of tidal volume and respiration rate. An 8-fold increase in tidal volume (250–2000 mL) decreased this size from 0.66 to 0.46 μm (minute volume of 15 L). Changing respiration rates also showed marked effects; changing from 3.75 to 30 breaths/min at 1000 mL tidal volume increased minimum deposition size from 0.46 to 0.58 μm, and deposition of 1.0 μm particles increased from 8% to 40%. The parameter that appeared to govern deposition fractions in the 0.1 to 3.2 μm size range was the average residence time of aerosols in the respiratory tract, involving diffusion and sedimentation. It was postulated that for particles with diameters between 0.4 and 2.9 μm, the rise in total deposition would primarily reflect the increased pulmonary deposition (*58*). At larger particle sizes, i.e., up to 8 μm, increasing flow rates caused increased total deposition, indicating deposition primarily by impaction; a transition to deposition primarily by sedimentation and diffusion occurred at approximately 4 μm (*25*).

In 1980, Stahlhoffen, Gebhart and Heyder (*64*) studied total deposition in human volunteers using Fe_2O_3 particles with ^{198}Au tracer; the numbers of inspired and expired particles were recorded automatically for each breath. Their results suggested that for particles up to 2.5 μm, deposition occurs only in the pulmonary lung under normal breathing conditions. They concluded that total deposition for particles less than 2.4 μm is due to sedimentation rather than impaction, unless volumetric flow rates are greatly increased; at particle diameters above 4.5 μm, alveolar deposition decreases very rapidly and the position of the maximum alveolar deposition is approximately 3 to 4 μm.

Theoretical curves shown in Figure 4 indicate that those of the TGLD for tidal volumes of 1450 and 750 mL are reasonably consistent with recent experimental results of a variety of authors, i.e., maximum deposition of nearly 100% for particle size diameters of 8 to 10 μm, and a minimum deposition of 20% at 0.2 to 0.5 μm. However, the theoretical curve of Yu et al. (*62*) provides a closer fit to the experimental points obtained by Chan and Lippmann (*51*), Heyder et al. (*58*), Lippmann and Albert (*47*) and Foord (*49*). At particle diameters below 0.2 μm, the TGLD curves rise very rapidly and depart radically from the available experimental data. All of these curves show considerably higher predicted deposition fraction than the actual data obtained by Swift et al. (*50*), suggesting an overestimate of deposition and a corresponding increase of chemical or radiological dose by factors of 2- to 4-fold.

Nasopharyngeal Deposition

The biological consequences of inhaled materials that are deposited in the nasopharynx during normal breathing can range from intermittent irritation and allergies to nasal carcinoma. Increased nasal cancer has appeard in several working populations that have persistently inhaled reactive airborne particles or materials that may adhere to particles, including leatherworkers (*65*), furniture makers (*66*), asbestos workers (*67*) and women employed as radium dial painters (*68*). Studies that describe the patterns and extent of inhaled particle deposition at various sites within the nasopharyngeal region are essential for determination of the potential toxicity of inhaled materials.

The first theoretical model of the deposition of inhaled particles of the nasopharyngeal region was developed in 1949 by Landahl and Tracewell (*69*) and predicted that deposition by impaction would predominate except for the lowest flow rates. Reasonable agreement with experimental data was obtained by passively aspirating through the nose and mouth of experimental subject aerosols of sodium potassium bicarbonate, corn oil, glycerol, tyrosine, bismuth subcarbonate and methylene blue (*69,70*). Pattle (*71*) in 1961 studied nasal deposition of monodispered methylene blue particles produced by a spinning disk generator. The fractional nasal penetration of inhaled particles was expressed by the empirical relationship:

$$P = 0.95[1 - 0.51 \log(D^2F/20.2)]$$

Here D is the particle diameter (μm) and F is the flow rate in liters/minute. Nasal deposition N for particles of a particular aerodynamic diameter (D_a) was expressed as:

$$N = -0.62 + 0.475 \log D_a^2F$$

This relationship was used by the TGLD to determine deposition in the nasopharyngeal region (*11*). Particles of the largest inhalable size (< 100 μm) down to about 20 μm were calculated to deposit quantitatively in the nasopharyngeal region. In 1971 Hounam et al. (*56*) developed equations for nasal deposition of inhaled insoluble particles and measured deposition in the nasopharynx N of pressure differential P_{nm} between nose and mouth:

$$N = -0.975 + 0.66 \log D_a^2P_{nm}$$

These data showed much less scatter rather than those obtained by Pattle (*71*) as a function of inspiratory air flow.

In 1970 Lippmann (*72*) measured nasal deposition as a function of particle aerodynamic diameter D_a and inspiratory flow F in volunteers who inhaled through the nose and exhaled through a mouthpiece, using normal breathing throughout; these data are shown in Figure 5. In 1974 Rudolph and Heyder (*73*) studied the nasal deposition of monodispersed aerosol particles, using four subjects with several tidal volumes, respiratory rates and patterns of exposure. Under the conditions of inhalation and exhalation in both directions through the nose and the mouth. Monodisperse particles (droplets) of di-2-ethyl-hexyl sebacate were used to determine nasal deposition as:

$$N = -0.63 + 0.51 \log D_a^2 F$$

This expression describes a curve having nearly the same slope as that of Pattle's empirical relationship (*71*), the latter shown by a straight line in Figure 5.

Individual variations in deposition and clearance may be extreme in this region. In 1973, Fry and Black (*57*) determined the regional deposition and clearance of particles in the human nose, finding up to 83% of inhaled particles of diameter 5, 7 or 10 μm deposited in regions of the nasopharynx that were characterized by biological clearance times of more than 12 hr. It thus may be necessary to examine clearance patterns for as much as 24 hr in some individuals in order to adequately characterize the movement and quantity of deposited particulate material.

Few experimental studies of the head deposition of particles, inhaled through the mouth, have been carried out with the proper equipment and with carefully regulated breathing patterns necessary to furnish reliable data. Exceptions are the classical studies of Lippmann (*72*), Chan and Lippmann (*51*) and Stahlhofen et al. (*64*). Lippmann (*72*) developed an external counting array of crystals surrounding the heads of volunteers who inhaled radionuclide-labeled aerosols. Data obtained from these studies, as well as the recent work of Chan and Lippmann (*51*) on 26 healthy nonsmokers and the results of Stahlhofen et al. (*64*) for mouth breathing in three subjects, are combined and shown as a single regression line in Figure 5, with confidence limits as presented in the recent study of Chan and Lippmann (*51*). Comparison of this composite curve for head deposition during mouth breathing with the individual data for deposition during nose breathing shows that much greater deposition is predicted in the nasopharynx during nose breathing than during mouth breathing. Conversely, breathing by mouth is likely to cause higher deposition fraction in the tracheobronchial region for a wide range of particle sizes.

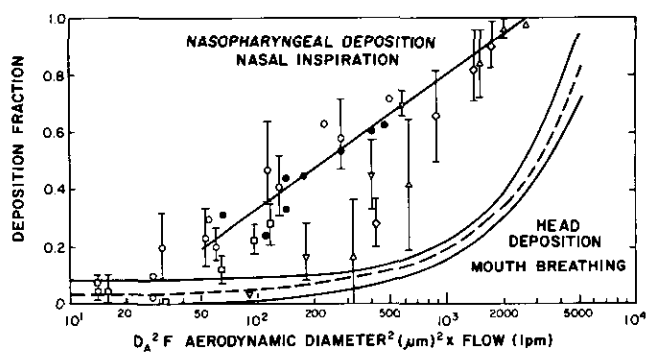

FIGURE 5. Deposition of inhaled particles in the nasopharynx during nose breathing and in the head during mouth breathing: (◇) Hounam et al. (*55*); (●) Lippmann (*47*), TV 1000 mL, 14 RPM; (○) Rudolf and Heyder (*73*); (□) Martens and Jacobi (*86*), TV 1000 mL, 14 RPM. The solid straight line is the empirical expression derived by Pattle (*71*) for deposition in the nasopharynx. Deposition in the head during mouth breathing is expressed as the dashed curve with confidence limits (solid boundary curves); it represents the combined data of Chan and Lippmann (*51*), TV 1000 mL, 14 RPM, and Stahlhofen et al. (*64*), TV 1500 mL, 15 RPM.

Heyder et al. (*25*) performed a series of experiments for both nose and mouth breathing using different respiratory flow rates, tidal volumes, and respiratory frequencies with a system that avoided respiratory pauses. Nasal deposition values showed much greater variability between subjects than did mouth breathing deposition, and that inertial impaction is likely to be much more efficient, particularly at high flow rates. At low flow rates, tidal volumes became very important; at 250 mL/sec, the particle size of minimum deposition dropped from 0.48 to 0.38 μm when the tidal volume was changed from 250 to 2000 mL. The authors concluded that the nose can be considered an effective "filter" that protects the rest of the respiratory tract.

A statistical description of aerosol particle deposition in the nose and mouth for inspiration and expiration has recently been developed in 1981 by Yu et al. (*74*). These authors have shown that the available data for nasal inspiration and expiration, as discussed above, fit well into two linear relationships in terms of log $\rho D^2 Q$ (where ρ is particle mass density, D is particle diameter and Q is flow rate), one for larger values of $\rho D^2 Q$, and the other for small values, i.e., ≤ 250 (g/μm³/sec), that correspond to submicron particles where diffusion deposition becomes important. In examining deposition during inspiration by mouth, all deposition values for $D^2 Q < 1000$ were essentially zero, indicating a single relationship was sufficient.

In addition to the high deposition probabilities for large particles in the nasopharynx during nasal breathing, this can be a very important region for diffusion deposition of fine particles as they first enter the respiratory tract (*72*). Information on the extent of deposition for very small particles (< 0.01 μm) within the nasopharynx is very limited. Hounam (*55*) found agreement between his experimental results and theoretical predictions (*69,70*), if he assumed that atmospheric condensation nuclei behaved as a uniform aerosol of about 0.01 μm median diameter; reasonable correlation was found between theoretical models and measured iodine vapor deposition in nose and mouth,

with 75 to 100% of the iodine vapor depositing in the nose and mouth.

If very small, rapidly diffusing particles act as carriers of attached radionuclides, their deposition can lead to severe pathology in this region. Freshly generated ^{106}Ru tetroxide attaches rapidly to available dust nuclei that deposit principally in the nasopharynx of large experimental animals (beagle dogs), causing highly localized irradiation of nasal epithelium (*75*). Daily exposures of 40 beagle dogs to alpha-emitting radon daughters attached to uranium ore dust particles (0.6–0.8 μm activity median aerodynamic diameter) caused a 25% incidence of respiratory tract carcinoma, with three cases of nasal carcinoma (*76*). Sprague-Dawley rats exposed to an atmosphere containing 16 to 20% of unattached radon daughters (very rapidly diffusing single ions) produced a high incidence of squamous metaphasia and squamous carcinoma in the nasopharynx (*76*). Rats exposed to radon daughters attached to more slowly diffusing dust particles that deposited at more distal sites in the respiratory tract showed no nasal carcinoma, but 60% incidence of squamous carcinoma and adenocarcinoma in the bronchioloalveolar lung (*60*). George et al. (*77*) found that both the size of the carrier uranium mine dust (or diesel exhaust) particles and the tidal volume influence nasal deposition of radon daughters in human subjects; larger particle sizes greatly increased penetration to regions beyond the nasopharynx.

Tracheobronchial Deposition

The tracheobronchial region of the respiratory tract extends from airway generation zero (trachea) to generation 16 (terminal bronchioles), i.e., the conducting airways beyond the larynx, where insoluble particles are cleared primarily via the mucociliary escalator. Experimental studies of tracheobronchial deposition patterns have been generally conducted in humans via mouth inhalation, bypassing much of the nasopharyngeal region. Recent studies have employed single-sized monodispersed aerosols with median diameters ranging from 0.1 to 8 μm. Lippmann and Albert (*47*) have established the technique of determining tracheobronchial deposition based on findings that tracheobronchial clearance via mucociliary transport appears to the complete within the first 24 hr after exposure. Exterior monitoring of the thorax for deposited monodispersed radiolabeled aerosols was used to determine the amount that is cleared during the first 24 hr; this was designated as the tracheobronchial deposition and is expressed as the fraction of aerosol entering the trachea that deposits in this region.

Extensive studies by Lippmann and Albert (*47*) and Lippmann et al. (*78*) (*54,79*) using monodispersed Fe_2O_3 spheres labeled with ^{198}Au or ^{51}Cr or ^{99m}Tc in humans and donkeys have provided data on deposition and clearance patterns within the tracheobronchial region of the respiratory tract. Large differences in tracheobronchial deposition fractions were found among individual human subjects. Deposition in this region during mouth breathing appears to be largely the result of impaction processes, particularly for particles greater than 4 μm aerodynamic diameter. Calculated deposition fractions for these sizes suggests that deposition should occur primarily by impaction within the first 10 to 12 airway generations (*78*). A transition in deposition mechanism from impaction to sedimentation was indicated beyond generation 12.

The TGLD (*11*) calculated that during nasal breathing the total tracheobronchial deposition fraction seldom exceeded 10% for aerosols having mass median diameters greater than 0.5 μm. A single figure of 8% was therefore used as a deposition value for all particle size distribution having mass median diameters between 20 and 0.02 μm. Morrow (*80*) has suggested that the mass deposition of the aerosol is likely to be controlled by larger particles undergoing inertial impaction in the bronchial tree, and that this is probably the major effect during mouth breathing because very few particles greater than 8 μm are able to penetrate the nose. In 1977 Lippmann et al. (*32*) reported that roughly 10% of inhaled particles with diameters as large as 15μm (aerodynamic) might penetrate into the tracheobronchial region during mouth breathing. Deposition of 1 to 5 μm diameter test particles was found to increase greatly in patients suffering from asthma or bronchitis, and was increased in cigarette smokers compared to nonsmokers (*32*).

Figure 6 presents the recent data obtained by several authors for tracheobronchial deposition as a function of particle size, studied in trained human volunteers using mouth breathing. Two fitted deposition curves de-

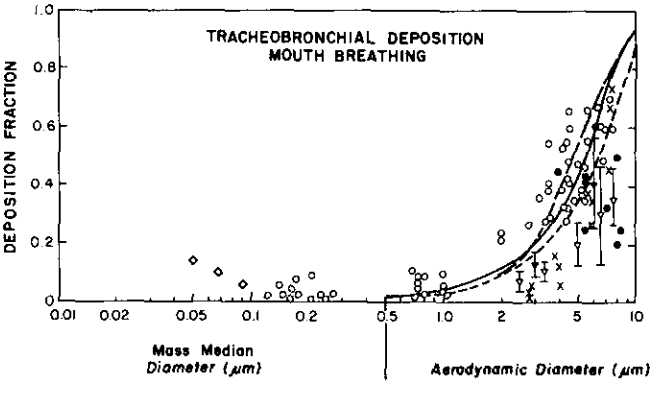

FIGURE 6. Deposition of inhaled particles in the tracheobronchial region of the respiratory tract during mouth breathing: (●) Lippmann and Albert (*47*), TV 750 mL, 14 RPM; (▼) Foord et al. (*49*), TV 1000 mL, 10 RPM; (▽) Foord et al. (*49*), TV 1000 mL, 15 RPM; (○) Chan and Lippmann (*51*), TV 1000 mL, 14 RPM; (–) Lippmann (*32*) fitted line to data from 26 volunteers; (×) Stahlhofen et al. (*64*), TV 1500 mL, 15 RPM; (◇) Nelson and Parker (*90*), TV ~ 1400 mL, 15 RPM; (——) Task Group on Lung Dynamics (*11*), TV 1450 mL, 15 RPM; (–) (*11*) TV 750 mL, 15 RPM.

scribed by Mercer (*81*) are included, based on TGLD calculations using 1450 and 750 mL tidal volumes (*11*), as well as the data collected by Lippmann (*32*) on 26 nonsmoking human volunteers. The data of Foord et al. (*49*) were obtained using tidal volumes of 1000 mL and 10 respirations or 15 respirations per minute. The data of Chan and Lippmann (*51*) are based upon studies involving an additional 26 volunteers who inhaled monodisperse particle sizes ranging from 7.5 to 0.12 μm. The results obtained by Stahlhofen et al. (*64*) on three subjects are also included. The generally lower values obtained in these studies may be due to the use of a constant respiratory flow rate instead of the variable flow rates used in the studies by Chan and Lippmann (*51*). Stahlhofen et al. (*64*) based their measurement of tracheobronchial deposition upon amounts cleared during the first week after inhalation.

The earlier work of Lippmann and Albert (*47*) established the dependence of tracheobronchial deposition upon an impaction parameter, defined as the square of the particle diameter times the flow rate. Palmes et al. (*82*) first attempted to classify populations of healthy individuals in regard to tracheobronchial deposition using an anatomic deposition parameter. In 1980, Chan and Lippmann (*51*) presented a new anatomical deposition parameter defined as the bronchial deposition size (BDS) and derived an expression for tracheobronchial deposition (TB):

$$TB = 8.14 \times 10^{-4}[D^2Q/(BDS)^3] + 0.037$$

Here Q is defined as the average inspiratory flow rate (liters per minute), and D is aerodynamic particle diameter (centimeters); in this empirical deposition model the tracheobronchial tree contained 16 generations of airways. Measurements of deposition in 26 nonsmokers, 46 cigarette smokers, 19 individuals having mild bronchitis, and 6 cases of severe bronchitis showed bronchial deposition sizes (BDS) of 1.20, 1.02, 0.90, and 0.60 cm for these groups, respectively, indicating the value of this analysis as a diagnostic tool to describe pulmonary disorders that affect the tracheobronchial region of the lungs. The authors describe bronchial deposition size as a deposition index; its magnitude represents a physical characterization of bronchial constriction in tracheobronchial airways based upon deposition measurements, and is therefore analogous to airway resistance as measured in pulmonary function tests.

Stahlhofen et al. (*64*), using monodisperse Fe_2O_3 particles labeled with ^{198}Au, showed tracheobronchial deposition values that were lower than those predicted by Lippmann (*32*) when expressed as a function of an impaction parameter D^2Q, where Q is the average inspiratory flow rate. In 1981 Cheng and Yeh (*83*) proposed a tracheobronchial deposition model based upon both impaction and sedimentation mechanisms. Mean deposition radii of 0.33 to 0.43 cm were obtained for three subjects, correlating with pulmonary functional residual capacities. These values were similar to calculated values of 0.263 and 0.376 cm based on equations from the lung model of Weibel (*14*) and the model of Yeh and Schum (*84*), respectively. Calculated contributions of sedimentation to tracheobronchial deposition were 42 to 78% at an inspiratory flow rate of 250 mL/sec, decreasing to 8 to 29% at an inspiration flow rate of 750 mL/sec; the latter corresponds well to the model of Chan and Lippmann (*51*), based on impaction alone, at the higher flow rate.

Figure 6 suggests that tracheobronchial deposition (principally by impaction) is the major mechanism for removal of inhaled large particles within the respiratory tract during mouth breathing. However, deposition values fall rapidly to a few percent for particles less than 1 μm MMAD. Chan and Lippmann (*51*) found tracheobronchial deposition values ranging between 1 and 10% for 1 to 0.1 μm particles during mouth breathing. The TGLD (*11*) calculated deposition values of $< 10\%$ for particle distributions having mass median diameters ranging from 10 to 0.1 μm during nasal breathing. Nasopharyngeal deposition by impaction was expected to remove most of the particles larger than 1 μm.

The foregoing discussion has described deposition patterns of particles of homogenous materials that may be used to evaluate a potential inhalation hazard, provided that particle size fractions are known. However, the high incidence of bronchogenic carcinoma among uranium miners (*85*) has focused attention on the deposition of the alpha-emitting daughter products of radon in selective regions of the tracheobronchial conducting airways, when attached to carrier particles of ore dust or diesel engine exhaust. Theoretical and experimental studies by Harley and Pasternack (*59*), Jacobi (*86*) and Parker (*87*), have shown that the subsegmental bronchi of the tracheobronchial airways are likely to receive the greatest radiological dose, due to selective deposition and rapid radioactive decay during subsequent biological clearance of inhaled radon daughters (^{218}Po, ^{214}Pb, ^{214}Bi, ^{214}Po). While comparatively few data exist for measured deposition of radon daughters based upon activity mass aerodynamic diameter, Nelson and Stuart (*88*) have demonstrated increased concentrations of deposited radon daughters at the bifurcations in the larger tracheobronchial airways, and Parker (*87*) has calculated composite deposition fractions in generations 0 to 16 of the respiratory tract, using Haque and Collison's (*89*) calculations based upon mouth breathing of attached radon daughters with inspiratory velocities of 347 mL/sec. Increasing deposition, largely due to diffusion within these airways, is indicated by the three values shown in Figure 6 for particle sizes of 0.09, 0.067 and 0.050 μm.

The increased deposition of alpha-emitting radionuclides in the tracheobronchial region during mouth breathing, caused by physical stress or impaired nasal breathing due to concomitant respiratory disease, may

be a major factor in the observed increase of bronchogenic carcinoma in uranium miners. Under these conditions i.e., obligatory mouth breathing, absorbed radiological doses due to deposition of radon daughters attached to carrier dust may increase by factors of three to five times, compared to breathing similar atmospheres via nasal inhalation (*90*).

Pulmonary Deposition

Insoluble particles that deposit in the alveolar or pulmonary region may cause accumulating injury to the lung, or may be gradually dissolved and transported to systemic organs via the blood or lymphatic channels. Predictive theoretical models have been made for pulmonary deposition using the same principles as described above for total deposition, but experimental verification of pulmonary deposition is much more difficult. Early studies, such as those by Wilson and LaMer (*26*), measured the quantities of inhaled and exhaled particles, and external monitoring of radioactively tagged materials. More recent studies, pioneered by Lippmann and Albert (*47*), have used radioactive tracer techniques involving inhalation of monodispersed particles by human volunteers. The amount of material deposited distal to the region of the ciliated airways and thus not cleared within the first 24 hr represented pulmonary or alveolar deposition. This was measured by external monitoring of the thorax.

The predictive curves and experimental data for pulmonary deposition of inhalation of particles that were developed between 1935 and 1950 are shown in Figure 7. Findeisen's (*36*) theoretical studies are shown in curves *1* and *2*. Curve *3* represents deposition calculated by Hatch and Hemeon (*91*), based upon studies by Van Wijk and Patterson (*46*) of inhaled dusts.

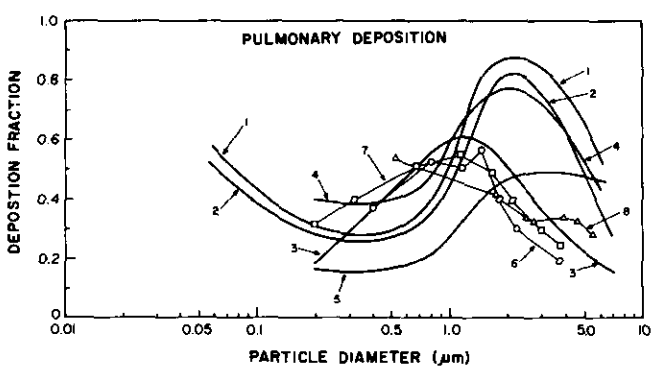

FIGURE 7. Predictive models and experimental values for pulmonary or alveolar deposition of inhaled particles: (1) predictive, Findeisen (*36*), 14 RPM, deposition distal to terminal bronchioles; (2) predictive, Findeisen (*36*), 14 RPM, depositions in alveolar ducts and alveoli; (3) predictive, Hatch and Hemeon (*91*); (4) predictive, Landahl (*21*), 300 mL/sec, 5 RPM, tidal volume 1350 mL, deposition in bronchioles and below; (5) predictive, Landahl (*21*), 15 RPM, tidal volume 450 mL, deposition below terminal bronchioles; (6) experimental, Wilson and LaMer (*26*) 5.5 RPM; (7) experimental, Brown et al. (*92*), 15 RPM, tidal volume 700 mL; (8) experimental, Gessner et al. (*93*).

Wilson and LaMer (*26*) examined pulmonary deposition during mouth breathing in subjects that inhaled monodispersed aerosols of glycerol and water, labeled with ^{128}sodium (curve *6*). In 1950 Brown et al. (*92*), measured pulmonary deposition in humans during nasal breathing of aerosols of china clay (curve *7*). Gessner et al. (*93*) examined the deposition of inhaled silica dust (curve *8*).

In 1965, Beeckmans (*40*) developed a predictive curve for pulmonary deposition based on Altshuler's (*94*) concept of interpulmonary gas mixing, with results similar to curves *2* and *4* of Figure 7. Increases were predicted in both total deposition and pulmonary deposition for particles < 0.10 μm, due primarily to diffusion. Altschuler et al. (*95*) in 1967 studied deposition of inhaled particles during mouth breathing by volunteers. After correction for mechanical aerosol mixing, their results indicated that the particle size for maximum alveolar deposition would be > 2 μm aerodynamic diameter. Davies (*96*) in 1967 examined the size distribution for dusts retained within the lungs and described particle size maximum to be < 1.5 μm. In 1971, Heyder and Davies (*52*) described a compartmental model influenced by changing tidal reserve volumes and residual air volumes, using particle exchange coefficients to predict the deposition of 0.5 μm particles in the lungs. They concluded that air mixing resulting from intertial flow and turbulence does not occur except in dead air space (conducting airway) regions, and that particle exchange is due to intrinsic motion of the particles. In 1972, Davies (*43*) described the fractions of inhaled particles that are deposited in alveolar air space as a function of particle size.

Figure 8 describes the deposition fractions for particles in the pulmonary lung as a function of aerodynamic or linear diameter, from data recently obtained during carefully controlled studies of human volunteers using mouth breathing. Chan and Lippmann (*51*) studied alveolar deposition during mouth breathing in 26 healthy nonsmokers, using a tidal volume of 1000 mL and 14 breaths/minute. Monodisperse Fe_2O_3 particles were tagged with ^{99m}Tc and ^{198}Au for assessment of deposition by external monitoring. Figure 8 also contains three predictive curves for pulmonary deposition. Two curves are based on calculations from the TGLD (*11*) at 15 breaths/minute, with tidal volumes of 1450 mL and 750 mL. The third curve was derived by Yu et al. (*62*) in 1978, based upon a two component theory for particle deposition (*63*). Particle concentrations in the conducting airways and in the alveolar region were considered to be different, and this difference in concentration caused a net mixing between tidal and residual aerosol during respiration. Yu (*63*) incorporated the effect of particle motion on aerosol mixing for steady mouth breathing without pause. The predictive deposition curves of Yu et al. (*62*) fit the data of Lippmann (*32*) very closely for larger particle sizes, with a pulmonary deposition of roughly 40% for 2 to 3 μm particles, at a tidal volume of 1000 mL and 14 respirations/minute. The TGLD model predicts higher maximum deposition

values of 50 to 60% for particles of 2 to 3 μm (*11*). All curves describe a minimum size for alveolar deposition between 0.2 and 0.5 μm, with depositions values of 12% predicted by the curve of Yu et al. (*62*), and 20% by the curves of the TGLD (*11*). Much better correspondence is evident between the data of Chan and Lippmann (*51*) and the recent theoretical treatment by Yu (*63*). No experimental data exist for pulmonary deposition of very fine particles, as it is very difficult to generate well-defined nonaggregated particle sizes < 0.1 μm. However, in this region the theoretical curve of Yu et al. (*62*) lies a factor of 2 to 4 below those predicted by the TGLD (*11*). The decreasing deposition below 0.02 μm is consistent with prior removal of rapidly diffusing small particles in proximal airways.

Heyder et al. (*27*) suggested in 1980 that volumetric flow rate was a major determinant of particle deposition by impaction, and that the effect of residence time within the lung was a primary determinant for particle deposition by sedimentation and diffusion. They conducted experiments using a mean volumetric flow rate constant of 250 mL/sec, and studied the effects of mean residence times of 2, 4 or 8 sec. Maximum alveolar deposition changed from 4 to 3.2 μm with increasing residence times. At 250 mL/sec, particles up to diameters of 2.4 μm were deposited almost entirely in the pulmonary region. At a mean flow rate of 750 mL/sec and a residence time of 2 sec, particles with diameters < 1.5 μm were apparently deposited only in the pulmonary region.

Associated experiments were conducted by Stahlhofen et al. (*64*) in 1980, using Fe_2O_3 monodispersed particles labeled with ^{198}Au radioactive tracer. Alveolar deposition was determined by extrathoracic scintillation counters, assuming rapid and quantitative removal of particles deposited in the tracheobronchial region. These investigators concluded that deposition of particle sizes < 2.4 μm (aerodynamic) occurs almost exclusively in the pulmonary region, under normal breathing conditions. This conclusion is supported by comparison of Figure 8 with that of total deposition for mouth breathing (Fig. 4), indicating virtually identical patterns of deposition for particle sizes up to 2.5 to 3.0 μm. Stahlhofen et al. (*64*) also suggested that because the flow velocity of the aerosol in the pulmonary region is too low to allow deposition by inertial impaction, deposition for particles of diameters < 2.4 μm is due almost entirely to gravitational sedimentation. For particles below 0.20 μm aerodynamic diameter, diffusion becomes the predominant mechanism of deposition in the pulmonary region as well as within the total respiratory tract; such deposition would increase with increasing mean residence times. The finding of rapid decrease in pulmonary deposition with increasing size for particles above 4.5 μm is amply supported by the data of Chan and Lippmann (*51*) and is well described by the predictive alveolar deposition curve developed by Yu et al. (*62*).

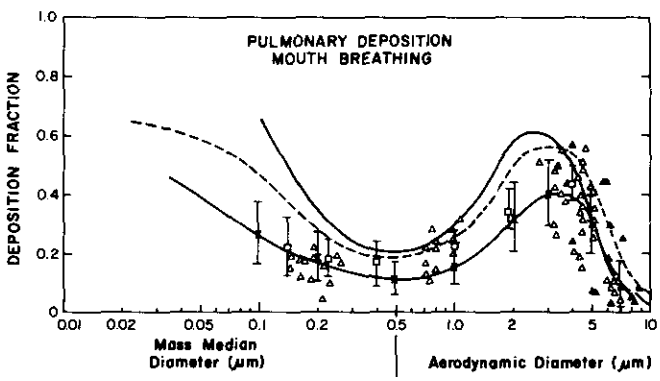

FIGURE 8. Deposition of inhaled particles in the pulmonary or alveolar region of the respiratory tract during mouth breathing: (▲) Lippmann and Albert (*47*), TV 1400 mL, 14 RPM; (□) Altshuler et al. (*95*), TV 500 mL, 15 RPM; (Δ) Chan and Lippmann (*51*), TV 1000 mL, 14 RPM; (—)Task Group on Lung Dynamics (*11*), TV 1450 mL, 15 RPM; (--) (*11*), TV 750 mL, 15 RPM; (×) Yu et al. (*62*), TV 1000 mL, 15 RPM; bars represent 3SD.

Mechanisms of Respiratory Tract Clearance

Particle Clearance Pathways

The clearance of inhaled deposited particles from the respiratory tract is a continuous process that entrains particles immediately upon their deposition. It consists of a complex set of processes involving the three principal regions of the respiratory tract described above, i.e., the nasopharynx, the tracheobronchial or conducting airways, and the pulmonary or gas exchange regions, all served to varying degrees by three primary routes of clearance; i.e., to the blood, to the lymphatic circulation and to the gastrointestinal tract. Insoluble materials that are deposited on inner airway surfaces of the nasopharyngeal or tracheobronchial regions of the respiratory tract may be cleared rapidly by mucociliary transport, either as intact particles or following phagocytosis by pulmonary alveolar macrophages. Insoluble particles that are deposited below the ciliated airways, i.e., beyond the terminal bronchioles may become a reservoir for subsequent translocation to other tissues via the bloodstream, to lymphatic channels draining into peripheral or hilar lymph nodes, or via gradual phagocytosis and conveyance within pulmonary macrophages to form a slow component of clearance into the gastrointestinal tract. Deposited particles composed of materials that are readily soluble may be absorbed into the bloodstream following dissolution within the airway lining fluids or cells. Clearance of soluble materials by this pathway may occur within all regions of the highly vascularized respiratory tract.

Mechanical Clearance Processes

Mucociliary Clearance of Airways. According to the classification of Jeffrey and Reid (*97*), there are

eight principal types of cells that form the respiratory epithelium. Among the six types of superficial cell (rather than basal and Kulchitski cells), five, including the goblet, serous, Clara, intermediate and brush cells, are nonciliated.

Goblet cells are found with varying density along the conducting airways of the respiratory tract and are responsible for the production of mucus that serves as a vehicle for entrapment and conveyance of deposited particles, propelled by the action of the cilia (*98*). In humans these cells produce sialomucin or a mixture of sulfomucin and sialomucin (*97*).

The serous cell is found in great numbers in proximal airways of specific pathogen free rats; it has recently been identified in fetal airways in man (*97*). It is responsible for serus secretions along the respiratory airway epithelium that may form a periciliary layer beneath the particle-bearing mucus.

Clara cells are found in airways as large as the trachea, but appear to be most frequent in the region of the terminal bronchioles (*99*). They apparently secrete a neutral glycoprotein and have subcellular structures similar to cells that are able to produce steroids (*100*).

Whether located in the nasopharynx or in the tracheobronchial airways, the ciliated cells propel mucus toward the oralpharynx, with subsequent clearance to the gastrointestinal tract. Ciliated cells of the upper respiratory tract each have about 200 cilia, with 8 to 10 projecting from each μm^2 of cell surface (*101*). Electron microscopic studies of the cilium have shown small clawlike projections at the tip that are thought to function in drawing the mucus forward (*102*). Cilia in the trachea have been reported by Dalhamn (*103*) to beat 1320 times/min, whereas Iravani (*104*) has found the frequency of ciliary beating in rats to range from 400 beats/min in the distal airways to about 1000 beats/min in the main lobar bronchi. This synchronized ciliary beating propels mucus at the rate of 0.4 mm/min in the smallest bronchioles up to nearly 12 mm/min in the lobar bronchi in rats (*99*), while rates of mucus movement in the dog range from 1.6 mm/min in small bronchioles to 4 mm/min in segmental bronchi and 12.6 mm/min in the trachea (*105*). Morrow et al. (*106*) calculate similar rates for movement of deposited particles in human lungs, i.e., 100 to 600 μm/min in the terminal bronchioles. Serafini et al. (*107*) found that much slower rates of movement occur at the periphery of the lung than in the proximal airways. Yeates et al. (*108*) and Wood et al. (*109*) describe flow rates of mucus in the human trachea of 5 to 20 mm/min.

There is little evidence of the buildup of fluids within the proximal airways of normal lungs during clearance, suggesting that reabsorption of the secretions from distal areas must take place. This is supported by the findings that secretions in peripheral airways are less viscous than those in central airways, as discussed by Asmundsson and Kilburn (*105*). Camner and Philipson (*110*) report that clearance by mucociliary action from the ciliated airways is likely to be complete within a matter of hours. The quality of mucus varies depending upon the location in the respiratory tract (*99*). In the distal and terminal bronchioles, the fluid lining of the airways consists primarily of a low viscosity serous fluid that is continuous with the surfactant lining the alveoli. The respiratory bronchioles are lined with nonciliated, or occasional low ciliated cells, with secretory cells and Clara cells becoming more numerous in toward the trachea. The next several generations of bronchioles are lined with ciliated epithelium that becomes continuous and is about 20 to 30 μm in depth, having few basal cells. In this region the ciliated cells cover about 50% of airway surface. Clara cells are sparse, but goblet cells that are capable of secreting more viscous mucus are more plentiful. In small airways the lining fluid lacks mucus, but goblet cells, found in greater density in the larger airways, produce mucus that becomes a continuous layer in the bronchi and trachea (*103*). The serous fluid lying beneath the mucus layer is subject to the action of cilia during both propulsion and return movement, but may not be propelled at the same velocity as the mucus layer (*99*). Mechanical clearance of insoluble particles, whether deposited directly upon this mucus layer, or within macrophages that are transported by the mucus layer, is the principal means of clearance to the gastrointestinal tract.

Deposition, retention and transport of radioactively labeled monodispersed aerosols in the respiratory tract have been studied extensively by Albert et al. (*111*), Camner et al. (*112*), and Lourenço et al. (*113*). Lippmann (*32*) has described a comprehensive series of studies of the mucociliary clearance of insoluble particles using labeled Fe_2O_3 microspheres inhaled by human volunteers. Bronchial clearance was found to vary between 3 to 24 hr, but subsequent clearance was a great deal slower and was thought to depend upon mechanisms other than mucociliary transport. Observed bronchial clearance tended to terminate rather abruptly, with little indication of a fast component of clearance from the alveoli. The pattern and magnitude of retention curves depended directly upon the size distribution of the deposited aerosol, the frequency and rate of inspiration, and the relative dimensions of the conducting airways. Therefore, the amount of material clearing within 24 hr, representing deposition in the tracheobronchial region, may vary greatly between subjects (*32*).

Yeates et al. (*108*) have used radiolabeled monodisperse aerosols to measure mean mucociliary transport rates of 4.7 ± 3 mm/min in 42 subjects, and 5.9 ± 3 mm/min in 14 subjects. Clarke and Pavia (*114*) have compared a variety of techniques used to measure tracheal mucus velocities in the lungs of man, including aerosols of radionuclides, cinebronchofiberscopy, roentgenography, and insufflated radio-opaque tantalum. Tracheal mucus velocities were found to be 5.8 ± 2.6 mm/min for older subjects, compared to 10.1 ± 3.5 mm/min for healthy young adult subjects (roentgenographic) (*115*) and 20.1 ± 6.3 mm/min (cinebroncho-

fiberscopy) (*109*) for another group of young subjects. Goodman et al. (*115*) have found that mucociliary clearance appears to slow with age, although there was no difference in clearance rates between men and women. Wong et al. (*116*) report that posture seems to have little effect on mucociliary clearance. Batemen et al. (*117*) have found that during sleep clearance is slowed; Clarke and Pavia (*114*) suggest that the slower clearance during sleep may be of importance in individuals suffering chronic bronchitis or asthma.

Clearance by the Pulmonary Alveolar Macrophage. Pulmonary macrophages are mobile cells that defend the lungs against bacterial or viral infection and are responsible for the initial collection and removal of deposited particles, particularly in the alveolar region of the lungs. They are able to phagocytize and lyse invading organisms, being rich in lysosomes that can attach to phagosomal membranes (*62*), surround ingested material and attack it with a variety of proteolytic enzymes (*118–120*). Brain (*121*) has pointed out that pulmonary alveolar macrophages can effectively reduce particle penetration through epithelial barriers and provide most of the bactericidal properties of the respiratory tract. These large mononuclear cells are found upon the alveolar surface, but are not a part of the continuous epithelial cell surface, which is composed of attenuated epithelial Type I pneumocytes and large alveolar cells, i.e., the Type II pneumocytes. In healthy mammals the precursor cells of the pulmonary alveolar macrophage are thought to be supplied by or reside in the pulmonary interstitium (*121*). When inhaled particles are deposited upon the respiratory epithelium, increased numbers of macrophages may be recruited from precursors in the lung, or may appear as a consequence of the increased multiplication of free pulmonary macrophages. It is also believed that they may derive from the bone marrow via blood monocytes.

Deposited particles that are removed by endocytosis, including phagocytosis, may follow a great variety of clearance patterns and/or half-times of removal, depending on their initial deposition site in the respiratory tract, the total amount deposited, their physicochemical properties, and the size, shape, and surface reactivity of the deposited particles. The clearance of insoluble dust from the pulmonary regions of the respiratory tract via the mucociliary escalator seems to occur rapidly following the appearance of dust in the macrophages (*122*). The pulmonary alveolar macrophage appears to translocate to airway regions of the lung that are lined with ciliated epithelium, allowing eventual clearance via the gastrointestinal tract. This process may play a predominant role in early clearance from the alveolar region, i.e., within the first few hours to several days (*121*). However, the process is not entirely effective, and the persistence of remaining toxic dust particles within this region, or continuing inhalation of toxic dusts, may lead to increased cellular damage or proliferation.

There is disagreement as to which of two pathways is primarily involved in removal of particle-bearing macrophages with ultimate transport to the gastrointestinal tract. The first pathway follows an interstitial route, whereas the second may be composed of a continuously moving surface film that in some way draws cells to the ciliated epithelium at terminal bronchioles. Brundelet (*123*), in studies of lungs from rats that inhaled dye particles, suggested that particle-containing macrophages may migrate to ciliated airways through lymphoid collections found at the bifurcations of major bronchi and bronchioles. Green (*124*), in studies of alveolar and bronchiolar transport mechanisms, observed collections of macrophages containing coal dust and suggested that alveolar lining fluid, alveolar cells and particles flowed within "liquid veins" between alveoli, with the driving force for such fluid flow derived from variations in the tension of the alveolar wall during the mechanics of respiration.

Movement of particle-bearing macrophages along the surface of the airways has been reported by Hatch and Gross (*6*). Ferin (*125*) exposed rats to aerosols of titanium oxide, a very inert dust, and studied localization of these particles within the lungs on days 1, 8 and 25 of exposure. Particle-bearing macrophages were found to be concentrated in alveolar ducts and at the junctions of the respiratory and terminal bronchioles. Much more rapid translocation of particles to the lymphatic system was observed as rats received increasing lung burdens of this material. Pulmonary clearance rates increased to several micrograms per day, reaching a plateau at a lung burden of almost 40 mg. This suggested that the physical mass of dust within the lung could affect the rates of lung clearance via pulmonary macrophages.

Toxic insoluble dusts may show a similar inhibiting effect upon macrophage clearance. LaFuma et al. (*126,127*) exposed rats to increasing air concentrations of ^{239}Pu oxide particles. They found that the initial or faster phase of lung clearance could be eliminated entirely at high levels of initially deposited plutonium. This may represent killing or immobilization of plutonium-bearing macrophages, leaving only a very protracted phase of clearance that may be due to gradual dissolution within the lung. Stuart et al. (*128*), in analyses of whole-body and pulmonary retention patterns for inhaled insoluble plutonium-239 oxide in large experimental animals, have found a similar disappearance of the early phases of phagocytic cell-mediated clearance. Less toxic particles, or particles in combination with toxic gaseous pollutants, may also have marked effects upon respiratory tract clearance. Phalen et al. (*129*) have found that ozone plus sulfate aerosols or ozone alone dramatically interfere with the early phase (0–50 hr) mucociliary transport, but can stimulate later clearance.

Brain (*130*) demonstrated that increased levels of particle deposition could stimulate an increase in the number of recoverable free cells within a few hours, attaining a maximum at about 1 day. In studies using

pulmonary lavage, rats exposed to a triphenyl phosphate submicron-sized aerosol at a mass concentration of 21 mg/m^3 showed an increase of 122% in such cells. Brain and Corkery (*131*) examined the degree of particle ingestion by macrophages obtained by successive pulmonary washings in hamsters exposed to colloidal ^{198}Au. They found that pre-exposure to Fe_2O_3 and colloidal carbon particles reduced the ingestion of the gold colloid by macrophages, when measured 2 hr after inhalation exposure. However, this uptake was within normal limits at the end of 24 hr. Pre-exposure to coal dust maintained a depression in gold colloid uptake, indicating a persistent detrimental effect of this material upon macrophage function. Strecker (*132*) examined rat lungs after inhalation of various types of dust, to determine the penetration of dust into pulmonary lymphatic channels and lymph nodes. Rats were exposed to aerosols of titanium, aluminum or ferric oxide dusts, and found that a mean pulmonary deposition of about 0.5 mg/lung caused little change in the number of pulmonary alveolar macrophages. However, a cytotoxic quartz dust at similar levels produced a very marked increase in the number and division rates of these cells (*132*).

Sorokin and Brain (*133*) described a prolonged phase of clearance of Fe_2O_3 that appeared at 1 to 3 weeks after exposure. Particles were found within macrophages of the connective tissue compartment of the respiratory tract. This localization of inhaled particles developed slowly over many months. Initially and for several months, the greatest portion of inhaled Fe_2O_3 particles were found within alveolar macrophages, but gradually the preponderance of retained material was found in connective tissue macrophages. Such macrophages laden with particles are apparently released very slowly from interstitial sites within the pulmonary parenchyma. Inhaled fibrogenic particles may be retained for even longer periods of time. Davis et al. (*134*) found greater levels of quartz in coal miners who had developed pulmonary massive fibrosis than those having earlier stages of simple pneumoconiosis.

Morgan et al. (*135*) exposed rats to aerosols of radioactively labeled asbestos fibers. They found that approximately 20 mg of these particles were retained within lungs, with little effect upon the number of free macrophages or their size. The incorporation of fibers by pulmonary alveolar macrophages was essentially complete within 24 hr. Thus, fibers that are considerably longer than the diameter of the pulmonary alveolar macrophage (10–12 μm) may accumulate in alveolar wall and are not likely to be susceptible to pulmonary lavage. Beck et al. (*136*) have suggested that the short fibers are not as damaging because they can be entirely engulfed by pulmonary macrophages, whereas the longer fibers can penetrate the alveolar macrophage membrane, causing release of proteolytic enzymes as well as loss of mobility or inactivation of these cells. Allison (*137*) has described a high correlation between the capacity of a variety of inhaled particles to induce lysosomal enzyme secretion from macrophages within culture and to induce pulmonary granulomas *in vivo*. Macrophage proteinases can also affect systems responsible for generation of kinin, blood coagulation and fibrinolysis (*133*).

Transport of Phagocytized or Free Particles to Regional Lymph Nodes

Inhaled particles that deposit and remain within the alveolar region of the lung can be transported via the lymphatic drainage system to regional lymph nodes (*124*). The relative toxicity of the inhaled material appears to influence this pathway. Ferin (*125*) found little accumulation of the inactive TiO_2 in thoracic lymph nodes of rats after 25 days. Sorokin and Brain (*133*) found that Fe_2O_3 particles accumulated only gradually in regional lymphatics. Thomas (*138*) developed a model to fit observed retention of inhaled particles in rats, hamsters and dogs. He found that inhaled plutonium oxide and other insoluble particles concentrated rapidly in the thoracic lymph nodes, exceeding the concentration within the lungs after three months. Stuart et al. (*139*), in analysis of deposition and translocation patterns of inhaled ^{239}Pu oxide particles in dogs, found that thoracic lymph nodes became the major secondary reservoir of translocated plutonium within the body. This secondary reservoir was responsible for the sigmoid accumulation of this radionuclide within the liver and skeleton and became the principal site for whole-body retention of this radionuclide at several years following a single inhalation exposure. Figure 9 describes the accumulation

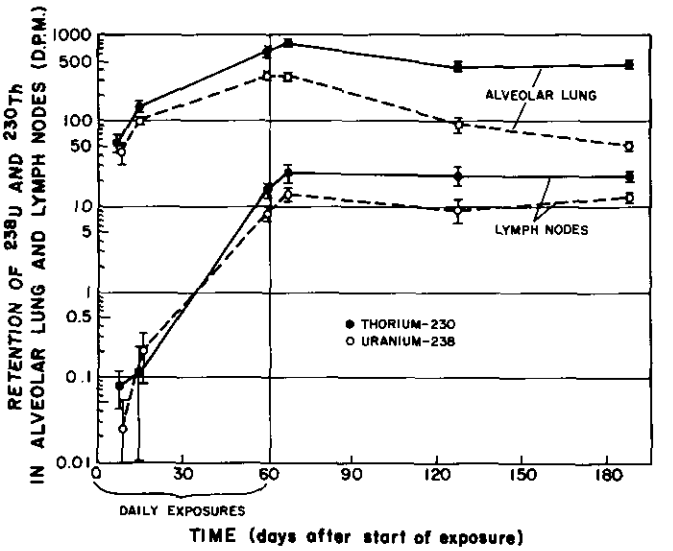

FIGURE 9. Accumulation and retention of uranium-238 and thorium-230 in the lungs and tracheobronchial lymph nodes of rats, when inhaled as constituents of uranium ore particles. Note the accumulations in the pulmonary lungs during daily exposures (4 hr/day), the translocation to regional lymph nodes, and the more rapid clearance by dissolution of the ^{238}U from the lungs after the cessation of exposures (*140*).

within the lungs of ^{238}U and ^{230}Th inhaled by rats as constituents of uranium ore, in studies reported by Stuart and Beasley (*140*). Radionuclide chemistry of these components of the highly insoluble uranium ore showed rapid accumulation within the lungs during 8 weeks of exposure, followed by translocation of both radionuclides, perhaps as intact particles, to the thoracic lymph nodes following cessation of exposures.

Dissolution of Inhaled Particles

Inhaled particles that are deposited upon respiratory tract epithelium may be subject to direct dissolution within the airway or alveolar lining fluids. Mercer (*141*) has developed a model for the dissolution of deposited materials, which in many cases appears to reasonably predict the disappearance rates of deposited materials within the lung. It was assumed that the deposited aerosol was log normal in particle size distribution, and that the deposited particles would gradually dissolve and disappear from the respiratory tract as a function of the surface area of each particle. This mode of clearance was described as a function of three parameters: (1) the median particle size of the mass distribution within the lungs after deposition, (2) a parameter related to the variability of the distribution, i.e., the geometric standard deviation, and (3) the nonequilibrium dissolution of the deposited material per unit of time. The latter parameter can be obtained by use of a synthetic dissolution medium having chemical properties similar to that of pulmonary interstitial fluid.

Thomas (*138*) has used this solubility model to estimate the size distribution of particles that were deposited in the alveolar lung of the rat, hamster and dog while studying the biological clearance of test materials in these animals. This dissolution model is based upon physicochemical characteristics of particle size and *in vitro* solubility, and appears to provide an adequate description of overall clearance rates for many soluble materials and some relatively insoluble particles that are deposited within the respiratory tract (*141*). However, such a model may provide little guidance in determining clearance fractions and half-times of materials tht are rapidly phagocytized and cleared primarily via a cell-mediated mechanism, either to the gastrointestinal tract or to regional lymph nodes.

Task Group on Lung Dynamics Clearance Model

The Task Group on Lung Dynamics (*11*) in 1966 proposed a model that defined various regions of the respiratory tract in order to predict inhaled particle retention based upon available data describing regional clearance mechanisms (Fig. 10). After inhaled particles are deposited, a fraction of the deposited material will pass either to the blood, to the gastrointestinal tract or to the lymphatic system, depending upon the observed or predicted retentions of the material, with the remainder described as being minimally retained, moderately retained or avidly retained (*142*). Pathway a represents a rapid clearance from the nasopharyngeal region to the bloodstream; pathway b represents clearance to the gastrointestinal tract (*11*). Pathways c and d represent clearance of the material deposited in the tracheobronchial region to the blood and to the gastrointestinal tract. The materials deposited in the pulmonary region are cleared by four pathways. Pathways f and g (rapid and protracted clearance) are followed by particles that proceed to the gastrointestinal tract after first being translocated through the tracheobronchial region via the mucociliary escalator. Pathway e represents clearance to the blood; pathway h represents clearance via the pulmonary lymphatic channels. Pathway i represents a movement of at least a portion of the material that accumulates in the regional lymph nodes and associated lymphatics to the bloodstream.

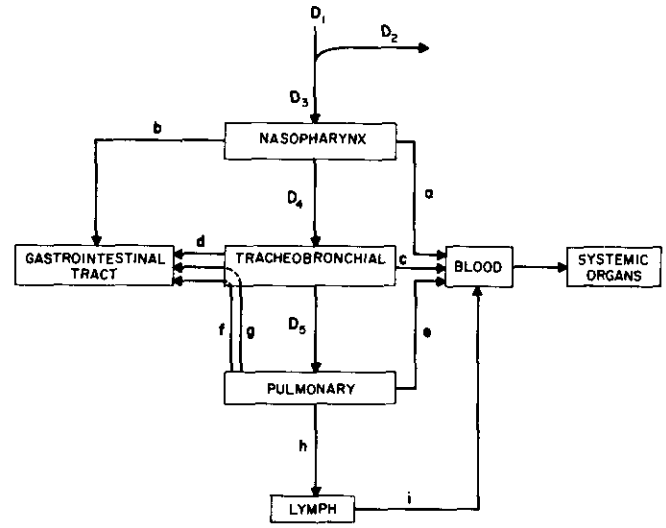

FIGURE 10. Deposition and clearance pathways for inhaled particles, following the predictive model of the Task Group on Lung Dynamics (*11*). Pathways (f) and (g) must pass through the tracheobronchial region. There may be more than one subcompartment representing "lymph," for insoluble materials, including retention in the thoracic and abdominal lymph nodes, depending upon physical chemical properties, total accumulated mass, and relative toxicity of the initially inhaled material.

Table 2 of the TGLD (*11*) was constructed by classifying materials as D, W and Y, signifying various fractions of deposited materials that are cleared with biological half-times of less than a day (D), materials having half-times for clearance of a few days to a few months (weeks, W) and half-times of a year or more (Y). Class Y materials are the oxides and hydroxides of most lanthanides and actinides, many of the carbides and lanthanide fluorides. Class W applies to materials of moderate retention, including a variety of sulfides and sulfates, carbonates, many phosphates, many of the hydroxides and oxides of chemical periodic table groups 2a, 3a, 4a, 5a, 6a, 8, 2b, 4b, 5, 6, and many of the halides and nitrates. Class D materials have minimal retention

Table 2. Constants for use with task group on lung dynamics clearance model.[a]

		Class (D)	Class (W)	Class (Y)
Nasopharynx	(a)	0.01/0.50	0.01/0.10	0.01/0.01
	(b)	0.01/0.50	0.4 /0.90	0.4 /0.99
Tracheobronchial	(c)	0.01/0.95	0.01/0.5	0.01/0.01
	(d)	0.2 /0.05	0.2 /0.5	0.2 /0.99
Pulmonary	(e)	0.5 /0.80	50/0.15	500/0.05
	(f)	n.a.	1.0 /0.40	1.0 /0.40
	(g)	n.a.	50/0.40	500/0.40
	(h)	0.5 /0.20	50/0.05	500/0.15
Lymph	(i)	0.5 /1.00	50/1.00	1000/0.90

[a] Values taken from the report of the Task Group on Lung Dynamics, ICRP Publication (*11*) and amended as in 1972 (*13*). The first value is the biological half-time in days; the second is the appropriate fraction. The single fraction of 0.90 listed for Class Y, pathway i, suggests a persistent reservoir for 10% of the material reaching the compartment.

and include many of the nitrates halides, phosphates, carbonates, sulfates and sulfides not included in Class W. There are several possible values for both the fractions and the half-times of Class Y materials proceeding by pathway i, i.e., material translocated from lungs through the regional lymph nodes which may eventually reach the systemic circulation (*13,138,139,*).

Nasopharyngeal Clearance

The TGLD model (*11*) assumed that rapid transport time would occur for all particles deposited in the nasopharynx. Although mucociliary clearance has been found to be rapid in some areas within the nasopharynx, there are other areas within this region that may be devoid of cilia, causing impaired clearance. Fry and Black (*57*) found that up to 83% of inhaled 2.5, 5, 7 or 10 μm particles were deposited in nasal regions that were cleared with biological half-lives of more than 12 hr. Clearance times on the order of a day or more in anterior unciliated regions may be the case in some individuals. Studies with nose-only inhalation of radionuclides by large experimental animals at the Inhalation Toxicology Research Institute (*143*) and at the Battelle, Pacific Northwest Laboratories (*144,145*) indicate retention times of several days or longer in the nasal turbinates of large experimental animals.

Tracheobronchial Clearance

Morrow (*80*) has suggested the use of three zones to describe tracheobronchial clearance, i.e., regions of conducting airways that are up to 10 cm, 10 to 20 cm, and 20 to 30 cm from the epiglottis. His experimental studies with radionuclide-labeled uniform 10 μm polystyrene particles and 7.5 μm mass median diameter iron oxide particles, using mouth breathing by humans and a multicrystal external detection system, indicated half-times of 0.5, 2.5 and 6 hr for the proximal, intermediate and peripheral regions, respectively. Tracheobronchial clearance was thus described by a three-component, six-parameter exponential expression. However, Morrow (*146*) pointed out that observed mucus velocities cannot readily be divided into convenient step gradients and developed in 1970 a model describing a continuous gradient of rates utilizing the data from many investigations. Tracheobronchial retention was described as an indirect function of the mass median diameter, in a form incorporating an initial value multiplied by an exponential power of time. It, too, was shown to be a reasonable approximation of the available data, although there is a wide degree of variability within the reported data itself. Albert et al. (*111*) have found wide intersubject variability in tracheobronchial clearance rates and fractions of nonsmoking volunteers, but that cigarette smoking may either decrease or increase rates depending on smoking history. Camner et al. (*112*) have also found wide individual variability in human tracheobronchial clearance rates (6 min to 1 hr), but much greater consistency in rates for the same individual in repeated studies using inhaled ^{18}Fl-labeled 7 μm particles.

Pulmonary Clearance

All of the pathways discussed above may be involved in the clearance of particles deposited within the pulmonary region of the lung. Endocytosis, including phagocytosis and pinocytosis, is a major clearance pathway of insoluble particles from the lung parenchyma. Macrophage transport may be the principal clearance mechanism from this region for insoluble materials, with cells migrating either via the tracheobronchial tree or via regional lymphatic channels. In addition, deposited particles that move directly to interstitial sites may be transported to the lymphatic vessels or blood capillaries, or may be phagocytized by macrophages in these regions. The particles entering lymphatic capillaries may become immobilized upon reaching the lymph nodes, and there serve as a secondary reservoirs for gradual input into the systemic circulation (*139*). Green (*124*) suggested that particle-bearing pulmonary macrophages may also migrate to subpleural and paraseptal positions, to perivascular sites or to peribronchiolar positions where nearly permanent storage in the lung may occur. These accumulations of particles within macrophages may form the initial lesions of chronic pulmonary diseases (*147*). However, a portion of the pulmonary burden of inhaled particles may be gradually removed by dissolution, resulting in the appearance of low concentrations of the material in the lymphatic or blood circulatory systems. The TGLD model (*11*) suggests that the physicochemical nature of the deposited particles determines their clearance pathways and rates of removal. However, this concept may not apply in cases of developing lesions or established lung pathology. In addition, Moss (*148*) and Moss and Kanapilly (*149*) have shown that rates of dissolution for individual components in an inhaled particle matrix may differ greatly.

The specific fractions and kinetics associated with

each clearance pathway must be re-evaluated as new information becomes available to validate the predictive use of such models. The possible alteration in clearance rates from the lung as a function of repeated versus single inhalation exposures to ^{144}Ce oxide on ^{239}Pu oxide is being studied at the Inhalation Toxicology Research Institute (*150*). In 1981 the Task Group on Respiratory Tract Kinetics of the National Council for Radiation Protection and Measurements (*151*) suggested that currently available clearance data can be used to define at least five major classes of compounds, instead of the three (D,W,Y) that served as the basis for the earlier TGLD model (*11*) described in Table 2. Brain and Valberg (*15*) have developed a comprehensive computer program based on the TGLD model to calculate particle retention and cumulative exposure to the respiratory tract. These authors urge caution in the application of such models, showing that changes in deposited particle size distributions and the relative solubility of a given material can alter retention and integrated dose in some compartments by as much as five orders of magnitude, even when identical total particle amounts are inhaled (*15*).

In 1980 Wilkey et al. (*152*) investigated mucociliary clearance of deposited particles in nine male subjects using monidisperse 7.9 μm (aerodynamic) Fe_2O_3 particles labeled with ^{99m}Tc. A gamma camera was used to study total bronchial clearance, as well as clearance from areas representing central (Zone I, generations 1–6), mid (Zone II, generations 7–13), and peripheral (Zone III, generations beyond 13) regions of the respiratory tract, defined for each subject from a series of bronchograms. Observed clearance rates were found to be in good agreement with the predictive model that the authors developed on the basis of the dichotomous branching system of Weibel (*14*). The mean half-times for total bronchial clearance and for clearance from the central, midregion, and peripheral regions were 1.90, 1.97, 1.70 and 2.62 hr, respectively (*152*). In comparison, Albert et al. (*153*) studied the deposition of 0.8 to 7.9 μm Fe_2O_3 particles in nine healthy subjects and found an average half-time for mucociliary clearance of 1.5 hr. Thomson and Short (*154*) reported an average mucociliary clearance of 2.8 hr for inhaled 5 μm polystyrene particles in five healthy subjects. Bohning et al. (*155*) found mean bronchial clearance half-times of 3.45 and 4.63 hr for Fe_2O_3 aerosols inhaled by male subjects, of whom some were cigarette smokers.

Conclusions

Theoretical and experimental investigations during the last few years have contributed greatly to defining the deposition of inhaled particles in the respiratory tract, with careful evaluation of the factors of size, density, shape, hydroscopicity, and charge that influence deposition in critical regions of the conducting airway and gas exchange regions of the lung. These studies have shown reasonable agreement between results of experimental tests and recent models, allowing prediction of deposition of fractions in order to assess the inhalation risks for many materials over a wide range of particle sizes. However, definitive studies are still needed to describe deposition of very small particles such as condensation nuclei that are produced during combustion (*147*). Inadequate data exist to evaluate a wide variety of air pollution hazards and to establish the risks that are associated with small particles (< 0.01 μm diameter) that serve as carriers for toxic gases or radioactive atoms such as radon or thoron daughters that may selectively irradiate sensitive respiratory epithelial cells, with potential to cause pulmonary carcinoma (*156*).

Nasal breathing versus mouth breathing can effectively protect the tracheobronchial region from very large particles and very small particles that may be removed in the nasal passages by impaction and diffusion, but resulting deposits in the pulmonary region may be significantly higher for mouth breathing than for nose breathing. This may be a critical change for persons doing heavy work or having impaired nasal airflows. Mouth breathing can cause 2- to 4-fold greater deposition in the region of subsegmental bronchi for very fine (< 1 mm) dust particles, (*90*), as well as increase tracheobronchial deposition of large particles (> 10 mm) to 25% or more.

There is a need for much more information on altered deposition and clearance patterns in persons suffering acute or chronic pulmonary diseases. In many abnormal conditions, tracheobronchial deposition may be increased, with a corresponding decrease in pulmonary deposition. The influences of age and biological variability upon particle deposition and clearance patterns are only beginning to be understood; wide differences in deposition patterns may occur among healthy young adults.

The available experimental results concerning clearance fractions and kinetics for particles deposited in different regions of the respiratory tract are continually expanding, but a great deal of additional data is needed to define normal clearance pathways, as well as the early and chronic effects of cigarette smoking. The extent to which overloading or cytotoxicity of certain materials may impair clearance pathways requires further study.

REFERENCES

1. Green, F. H. Y., Bowman, L., Castranova, V., Dollberg, D. D., Elliott, J. A., Fedan, J. S., Hahon, N., Judy, D. J., Major, P. C., Mentnech, M. S., Miles, P. R., Mull, J., Olenchock, S., Ong, T., Pailes, W. M., Resnick, H., Stettler, L. E., Tucker, J. G., Vallyathan, V., and Whong, W. Health implications of the Mount St. Helens volcano: laboratory investigations. Ann. Occup. Hyg. 26: 921–923 (1982).
2. Dibner, B. Agricola on metals. In: De Re Metallica, Agricola, 1556. Burnby Library, Norwalk, CT, 1958.
3. Drinker, P., and Hatch, T. F. Industrial dust. McGraw-Hill, New York, 1954.
4. Ludwig, P., and Lorenzer, E. Untersuchung der Grubenluft in

den Scheeberger Gruben auf den Gehalten Radiumenanation. Strahlentherapie 7: 428–435 (1924).
5. Watkins-Pitchford, W., and Moir, J. On the nature of the doubly refracting particles seen in microscopic sections of silicotic lungs, and an improved method for disclosing siliceous particles in such sections. S. Afr. Inst. Med. Res. 1: 207–230 (1916).
6. Hatch, T., and Gross, P. Pulmonary Deposition and Retention of Inhaled Aerosols. Academic Press, New York, 1964.
7. Amdur, M. O., and Underhill, D. The effect of various aerosols on the response of guinea pigs to sulfur dioxide. Arch. Environ. Health 16: 460–468 (1968).
8. Silverman, L., Billings, C. E., First, M. W., and Dennis, R. Air flow measurements on human subjects with and without respiratory resistance at several work rates. Arch. Ind. Hyg. Occup. Med. 3: 461–478 (1951).
9. Dautrebande, L. Microaerosols. Academic Press, New York, 1962.
10. Green, H. L., and Lane, W. R. Particulate Clouds: Dusts, Smokers, and Mists. D. Van Nostrand, Princeton, N.J., 1957.
11. Morrow, P. E., Bates, D. V., Fish, B. R., Hatch, T. F., and Mercer, T. T. International commission on radiological protection task group on lung dynamics; deposition and retention models for internal dosimetry of the human respiratory tract. Health Phys. 12: 173–207 (1966).
12. Holmes, T. H., Goodell, H., Wolf, S., and Wolff, H. G. The Nose. Charles C Thomas, Springfield, IL, 1950.
13. International Commission on Radiation Protection. The metabolism of Compounds of Plutonium and Other Actinides (ICRP Publication 19) Pergamon Press, Oxford, 1972, p. 6.
14. Weibel, E. R. Morphometry of the Human Lung. Springer Verlag, Berlin, 1963.
15. Brain, J. D., and Valberg, P. A. Models of lung retention based on ICRP task group report. Arch. Environ. Health 28: 1–11 (1974).
16. Landahl, H. D. Particle removal by the respiratory system: note on the removal of airborne particulates by the human respiratory tract with particular reference to the role of diffusion. Bull. Math. Biophys. 25: 29–39 (1963).
17. Morrow, P. E. Lymphatic drainage of the lungs in dust clearance. In: International Conference on Coal Workers' Pneumoconiosis. New York Academy of Sciences, New York, 1971.
18. Stuart, B. O. Selection of animal models for evaluation of inhalation hazards in man. In: Air Pollution and the Lung: Proceedings Twentieth Annual OHOLO Biological Conference (E. F. Aharonson, A. Ben-David and M. A. Klingberg, Eds.), John Wiley and Sons, New York, 1975, pp. 268–288.
19. Silverman, L., and Billings, C. E. Pattern of air flow in the respiratory tract. In: Inhaled Particles and Vapours (C. N. Davies, Ed.), Pergamon Press, London, 1961, pp. 9–45.
20. Morrow, P. E. Some physical and physiological factors controlling the fate of inhaled substances. I. Deposition. Health Phys. 2: 366–378 (1960).
21. Landahl, H. D. On the removal of airborne droplets by the human respiratory tract. I. The lung. Bull. Math. Biophys. 12: 43–56 (1950).
22. Cunningham, E. On the velocity of steady fall of spherical particles through fluid medium. Proc. Roy. Soc. (London) A83: 357–365 (1910).
23. Davies, C. N. Definite equations for the fluid resistance of spheres. Proc. Phys. Soc. 57: 259–270 (1945).
24. Morrow, P. E. Evaluation of inhalation hazards based upon the respirable dust concept and the philosophy and application of selective sampling. Am. Ind. Hyg. Assoc. J. 25: 213–236 (1964).
25. Heyder, J., Gebhart, J., and Stahlhofen, W. Inhalation of aerosols. Particle deposition and retention. In: Generation of Aerosols and Facilities for Exposure Experiments (K. Willeke, Ed.), Ann Arbor Science, Ann Arbor, MI, 1980, pp. 65–103.
26. Wilson, I. B., and La Mer, V. K. The retention of aerosol particles in the human respiratory tract as a function of particle radius. J. Ind. Hyg. Toxicol. 30: 265–280 (1948).
27. Dautrebande, L., and Walkenhorst, W. New studies on aerosols XXIV. Arch. Int. Pharmacodyn. 162: 194 (1966).
28. Raabe, O. G. Deposition and Clearance of Inhaled Aerosols. U. S. Department of Energy, National Technical Information Service, UCD-472-503, Springfield, VA, 1979.
29. Sinclair, D., Countess, R. J., and Hoopes, G. S. Effect of relative humidity on the size of atmospheric aerosol particles. Atmospheric Environment 8: 111–117 (1974).
30. Timbrell, V., and Skidmore, J. W. The effect of shape on particle penetration and retention in animal lungs. In: Inhaled Particles, Vol. III (W. H. Walton, Ed.), Unwin Brothers, Surrey, England, 1971, pp. 49–57.
31. Beeckmans, J. M. Deposition of ellipsoidal particles in the human respiratory tract. In: Assessment of Airborne Particles (T. T. Mercer, P. E. Morrow and W. Stober, Eds.), Charles C Thomas, Springfield, IL, 1972, pp. 361–367.
32. Lippmann, M. Regional deposition of particles in the human respiratory tract. In: Handbook of Physiology, Section 9: Reactions to Environment Agents (D. H. K. Lee, H. L. Falk and S. D. Murphy, Eds.), American Physiological Society, Bethesda, MD, 1977, pp. 213–232.
33. Mercer, T. T. Aerosol Technology in Hazard Evaluation. Academic Press, New York-London, 1973.
34. Melandri, C., Prodi, V., Tarroni, G., Famignani, M., De Ziacomo, T., Bompani, G. F., and Maestri, G. On the deposition of unipolarly charged particles in the human respiratory tract. In: Inhaled Particles, Vol. IV (W. H. Walton, Ed.), Pergamon Press, Oxford, pp. 193–201.
35. Vincent, J. H., Johnston, W. B., Jones, A. D., and Johnston, A. M. Static electrification of airborne asbestos: a study of its causes, assessment and effects on deposition in the lungs of rats. Am. Ind. Hyg. Assoc. J. 42: 711–721 (1981).
36. Findeisen, W. Uber das Absetzen kleiner, in der Luft suspendierten Teilchen in der menschlichen Lunge bei der Atmung. Pflugers Arch. Ges. Physiol. 236: 367–379 (1935).
37. Landahl, H. D., Tracewell, T. N., and Lassen, W. H. On the retention of airborne particulates in the human lungs. Arch. Ind. Hyg. Occup. Med. 3: 356–366 (1951).
38. Sinclair, D., and LaMer, V. K. Light scattering as a measure of particle size in aerosols: the production of monodispersed aerosols. Chem. Rev. 44: 245–267 (1949).
39. Altschuler, B., Yarmus, L., and Palmes, E. D. Aerosol deposition in the human respiratory tract. Arch. Ind. Health 15: 293–303 (1957).
40. Beeckmans, J. M. The deposition of aerosols in the respiratory tract. (1) Mathematical analysis and comparison with experimental data. Can. J. Physiol. Pharmacol. 43: 157–172 (1965).
41. Dennis, W. L. A formalized anatomy of the human respiratory tract. In: Inhaled Particles and Vapours (C. N. Davies, Ed.), Pergamon Press, London, 1961, pp. 88–94.
42. Walkenhorst, W., and Dautrebande, L. Uber die Retention von Kochalzteilchen in der Atemwegen. In: Inhaled Particles and Vapours (C. N. Davies, Ed.), Pergamon Press, London, 1961, pp. 110–121.
43. Davies, C. N. An algebraic model for the deposition of aerosols in the human respiratory tract during steady breathing. J. Aerosol. Sci. 3: 297 (1972).
44. Report of ICRP Committee 2 on permissible dose for internal radiation. Health Phys. 3: 173–207 (1960).
45. Gormley, P. G., and Kennedy, M. Diffusion from a stream flowing through a cylindrical tube. Proc. Roy. Irish Acad. A52: 163–169 (1949).
46. Van Wijk, A. M., and Patterson, H. S. The percentage of particles of different sizes removed from dust-laden air by breathing. J. Ind. Hyg. Toxicol. 22: 31–35 (1940).
47. Lippmann, M., and Albert, R. The effect of particle size on the regional deposition of inhaled aerosols in the human respiratory tract. Am. Ind. Hyg. Assoc. J. 30: 257–275 (1969).
48. Giacomelli-Maltoni, G., Melandri, C., Prodi, V., and Tarroni, G. Deposition efficiency of monodisperse particles in human respiratory tract. Am. Ind. Hyg. Assoc. J. 33: 603–610 (1972).
49. Foord, N., Black, A., and Walsh, M. Regional deposition of 2.5–7.5 micrometer diameter inhaled particles in healthy male nonsmokers. J. Aerosol Sci. 9: 343–357 (1978).

50. Swift, D. L., Stanty, F., and O'Neil, J. T. Human respiratory deposition patterns of fume-like particles. Presented in part at the 1977 American Industrial Hygiene Conference, New Orleans, LA, 1977.
51. Chan, T. L., and Lippmann, M. Experimental measurements and empirical modelling of the regional deposition of inhaled particles in humans. Am. Ind. Hyg. Assoc. J. 41: 399–409 (1980).
52. Heyder, J., and Davies, C. N. The breathing of half micron aerosols: III. Dispersion of particles in the respiratory tract. J. Aerosol Sci. 2: 437–452 (1971).
53. George, A. C., and Breslin, A. J. Deposition of radon daughters in humans exposed to uranium in atmospheres. Health Phys. 17: 115–124 (1969).
54. Holleman, D. F., Martz, D. E., and Schiager, K. J. Total respiratory deposition of radon daughters from inhalation of uranium mine atmospheres. Health Phys. 17: 187–198 (1969).
55. Hounam, R. F. The deposition of atmospheric condensation nuclei in the nasopharyngeal region of the human respiratory tract. Health Phys. 20: 219–220 (1971).
56. Hounam, R. F., Black, A., and Walsh, M. The Deposition of aerosol particles in the nasopharyngeal region of the human respiratory tract. In: Inhaled Particles, III (W. H. Walton, Ed.), Unwin Brothers Limited, Surrey, 1971, pp. 71–80.
57. Fry, F. A., and Black, A. Regional deposition and clearance of particles in the human nose. J. Aerosol Sci. 4: 113–124 (1973).
58. Heyder, J., Arbruster, L., Gebhart, J., Grein, E., and Stahlhofen, W. Total deposition of aerosol particles in the human respiratory tract for nose and mouth breathing. J. Aerosol Sci. 6: 311–328 (1975).
59. Harley, N. H., and Pasternack, B. S. Alpha absorption measurements applied to lung dose from radon daughters. Health Phys. 23: 771–782 (1972).
60. Stuart, B. O., Willard, D. A., and Howard, E. B. Uranium mine air contaminants in dogs and hamsters. Inhalation Carcinogenesis AEC (Symposium Series 18), Gatlinburg, TN, 1970, pp. 413–428.
61. Palmer, H. E., Perkins, R. W., and Stuart, B. O. The distribution and deposition of radon daughters attached to dust particles in the respiratory system of humans exposed to uranium mine atmospheres. Health Phys. 10: 1129–1135 (1964).
62. Yu, C. P., Nicolaides, P., and Soong, T. T. Effect of random airway sizes on aerosol deposition. Am. Ind. Hyg. Assoc. J. 40: 999–1005 (1979).
63. Yu, C. P. A two component theory of aerosol deposition in human lung airways. Bull. Math. Biol. 40: 693–706 (1978).
64. Stahlhofen, W., Gebhart, J., and Heyder, J. Experimental determination of the regional deposition of aerosol particles in the human respiratory tract. Am. Ind. Hyg. Assoc. J. 41: 385–398 (1980).
65. Acheson, E. D. Nasal cancer in the furniture and boot and shoe manufacturing industries. Prev. Med. 5: 295–315 (1976).
66. Andersen, H. C., Andersen, I., and Solgaard, J. Nasal cancers, symptoms and upper airway function in woodworkers. Brit. J. Ind. Med. 34: 201–207 (1977).
67. Stell, P. M., and McGill, T. Asbestos and cancer of the head and neck. Lancet i: 678 (1973).
68. Sharpe, W. D. Chronic radium intoxication: clinical and autopsy findings in long-term New Jersey survivors. Environ. Res. 8: 243–383 (1974).
69. Landahl, H. D., and Tracewell, T. Penetration of airborne particulates through the human nose. J. Ind. Hyg. Toxicol. 31: 55–59 (1949).
70. Landahl, H. E., and Black, S. Penetration of airborne particulates through the human nose. J. Ind. Hyg. Toxicol. 29: 269–277 (1947).
71. Pattle, R. E. Retention of gases and particles in the human nose. In: Inhaled Particles and Vapours (C. N. Davies, Ed.), Pergamon Press, London, 1961, pp. 302–314.
72. Lippmann, M. Deposition and clearance of inhaled particles in the human nose. Ann. Otol. Rhinol. Laryngol. 79: 519–528 (1970).
73. Rudolf, G., and Heyder, J. Deposition of aerosol particles in the human nose. In: Aerosole in Naturwissenschaft, Medizin und Technik (Proceedings of a Conference held in Bad Soden, October 16–19, 1974) (V. Bohlan, Ed.), Gesellschaft fur Aerosolforschung, Bad Soden, West Germany, 1974.
74. Yu, C. P., Diu, C. K., and Soong, T. T. Statistical analysis of aerosol deposition in nose and mouth. Am. Ind. Hyg. Assoc. J. 42: 726–733 (1981).
75. Snipes, M. B. Deposition, retention and dosimetry of inhaled ^{106}Ru attached to inert particles. In: Inhalation Toxicology Research Institute Annual Report 1978–1979, LF-69, UC-48, 43–48. Lovelace Biomedical and Environmental Research Institute, Albuquerque, NM, 1979.
76. Stuart, B. O. Studies of inhaled radon daughters in laboratory animals. In: Radon and Radon Daughters Exposures in the U.S. (Report to Scientific Committee 57, National Council on Radiation Protection and Measurements) (N. Harley, Ed.), 1981.
77. George, A. C., Hinchliffe, L., Epps, R., and Shepich, T. J. Respiratory tract deposition of radon daughters in humans exposed in a uranium mine (Phase III), 70–7, U. S. Atomic Energy Commission, New York Operations Office, New York, New York, 1970.
78. Lippmann, M., Albert, R. E., and Peterson, H. T., Jr. The regional deposition of inhaled aerosols in man. In: Inhaled Particles, Vol. III (W. H. Walton, Ed.), Unwin Brothers Limited, Surrey, England, 1971, pp. 105–120.
79. National Academy of Sciences, Committee on Medical and Biological Effects of Environmental Pollutants. Ozone and Other Photochemical Oxidants. National Academy of Sciences, Washington, DC, 1977.
80. Morrow, P. E. Theoretical and experimental models for dust deposition and retention in man. UR-3490-169, University of Rochester, Rochester, NY, 1972.
81. Mercer, T. T. The deposition model of the Task Group on Lung Dynamics: a comparison with recent experimental data. Health Phys. 29: 673–630 (1975).
82. Palmes, E. D., Nelson, N., and Lippmann, M. Effect of chronic obstructive pulmonary disease on rate of deposition of aerosols in the lung during breathholding. In: Inhaled Particles Vol. III (W. H. Walton, Ed.), Unwin Bros. Ltd., Surrey, England, 1971, pp. 123–130.
83. Cheng, Y. S., and Yeh, H. C. A model for aerosol deposition in the human tracheobronchial region. Am. Ind. Hyg. Assoc. J. 42: 771–776 (1981).
84. Yeh, H. C., and Schum, G. M. Models of human lung airways and their application to inhaled particle deposition. Bull. Math. Biol. 42: 461–480 (1980).
85. Archer, V. E., Wagoner, J. K., and Lundin, F. E. Lung cancer among uranium miners in the United States. Health Phys. 25: 351–372 (1973).
86. Jacobi, W. Relations between the inhaled potential alpha-energy of ^{222}Rn and ^{220}Rn decay products. Health Phys. 10: 1163–1175 (1972).
87. Parker, H. M. The dilemma of lung dosimetry. Health Phys. 16: 553–562 (1969).
88. Nelson, I. C., and Stuart, B. O. Radon daughter deposition in the respiratory tract. In: Battelle Pacific Northwest Laboratory Annual Report for 1970 to USAEC Division of Biology and Medicine, Vol. II, Part 2. U. S. Energy Research and Development Administration, Germantown, MD, 1971, pp. 67–68.
89. Haque, A. K. M., and Collinson, A. J. L. Radiation dose to the respiratory system due to radon and its daughter products.
90. Nelson, I. C., and Parker, H. M. A Further Appraisal of Dosimetry Related to Uranium Mining Health Hazards. National Institute for Occupational Safety and Health, Cincinnati, OH, 1974.
91. Hatch, T., and Hemeon, W. L. C. Influence of particle size in dust exposure. J. Ind. Hyg. Toxicol. 30: 172–180 (1948).
92. Brown, J. H., Cook, K. M., Ney, F. G., and Hatch, T. Influence of particle size upon the retention of particulate matter in the human lung. Am. J. Public Health 40: 450–458 (1950).
93. Gessner, H., Ruttner, J. R., and Buhler, H. Zur Bestimmung des Korngrossenbereiches von silikogenem Staub. Schweiz.

Med. Wochenschr. 79: 1258–1262 (1949).
94. Altshuler, B. The role of the mixing of intrapulmonary gas flow in the deposition of aerosols. In: Inhaled Particles and Vapours (C. N. Davies, Ed.), Pergamon Press, Oxford, 1961, pp. 47–53.
95. Altshuler, B., Palmes, E. D., and Nelson, N. Regional aerosol deposition in the human respiratory tract. In: Inhaled Particles and Vapours, Vol. II (C. N. Davies, Ed.), Pergamon Press, Oxford, 1967, pp. 323–338.
96. Davies, C. N. In: Inhaled Particles and Vapours, Vol. II (C. N. Davies, Ed.), Pergamon Press, Oxford, England, 1967, preface.
97. Jeffery, P. K., and Reid, L. M. The respiratory mucous membrane. In: Respiratory Defense Mechanisms, Part I (J. D. Brain, D. F. Proctor, and L. M. Reid, Eds.), Marcel Dekker, New York, 1977, pp. 193–238.
98. Schulze, F. E. The lungs: 1. The lungs of mammals. In: Human and Comparative Histology (S. Stricker, Ed.; H. Power, transl.), New Sydenham Soc., London, 1972, pp. 49–68.
99. Sleigh, M. A. The nature and action of the respiratory tract cilia. In: Respiratory Defense Mechanisms, Part I (J. D. Brain, D. F. Proctor and L. M. Reid, Eds.), Marcel Dekker, New York, 1977, pp. 247–288.
100. Cutz, E., and Conen, P. E. Ultrastructure and cytochemistry of Clara cells. Am. J. Pathol. 62: 127–142 (1971).
101. Rhodin, J. Ultrastructure and function of the human tracheal mucosa. Am. Rev. Respir. Dis. 93: 1–15 (1966).
102. Jeffery, P. K., and Reid, L. M. New features of rat airway epithelium a quantitative and electron-microscopic study. J. Anat. 120: 295–320 (1975).
103. Dalhamn, T. Mucous flow and ciliary activity in the trachea of healthy rats and rats exposed to respiratory irritant gases. Acta Physiol. Scand. (Suppl. 123) 36: 1–163 (1956).
104. Iravani, J. Flimmerbewegung in den intrapulmonalen Luftwegene der Ratte. Pflugers Arch. 297: 221–237 (1967).
105. Asmundsson, T., and Kilburn, K. H. Mucociliary clearance rates at various levels in dogs lungs. Am. Rev. Respir. Dis. 102: 388–397 (1970).
106. Morrow, P. E., Gibb, F. R., and Gazioglu, K. M. A study of particulate clearance from the human lungs. Am. Rev. Respir. Dis. 96: 1209–1221 (1967).
107. Serafini, S. M., Wanner, A., and Michaelson, E. D. Mucociliary transport in central and intermediate size airways and effect aminophyllin. Bul. Eur. Physiopath. Respir. 12: 415–422 (1976).
108. Yeates, D. B., Aspin, N., Levison, H., Jones, M. T., and Bryan, A. C. Mucociliary tracheal transport rates in man. J. Appl. Physiol. 39: 487–495 (1975).
109. Wood, R. E., Wanner, A., Hirsch, J., and Farrell, P. M. Tracheal mucociliary transport in patients with cystic fibrosis and its stimulation by terbutaline. Am. Rev. Respir. Dis. 111: 733–738 (1975).
110. Camner, P., and Philipson, K. Human alveolar deposition of 4 um teflon particles. Arch. Environ. Health 36: 181–185 (1978).
111. Albert, R. E., Lippmann, M., Peterson, H. T., Berger, J., Sanborn, K., and Bohning, D. Bronchial deposition and clearance of aerosols. Arch. Intern. Med. 131: 115–131 (1973).
112. Camner, P., Philipson, K., Friberg, L., Holma, B., Larsson, B., and Svedberg, J. Human tracheobronchial clearance studies. Arch. Environ. Health 22: 444–449 (1971).
113. Lourenco, R. V., Loddenkemper, R., and Cargon, R. W. Patterns of distribution and clearance of aerosols in patients with bronchiectasis. Am. Rev. Respir. Dis. 106: 857–866 (1972).
114. Clarke, S. W., and Pavia, D. Lung mucus production and mucociliary clearance: methods and assessment. Brit. J. Clin. Pharmacol. 9: 537–546 (1980).
115. Goodman, R. M., Yergen, B. M., Landa, J. F., Golinvaux, M. H., and Sackner, M. A. Relationship of smoking history and pulmonary function tests to tracheal mucus velocity in nonsmokers, young smokers, ex-smokers, and patients with chronic bronchitis. Am. Rev. Respir. Dis. 117: 205–214 (1978).
116. Wong, J. W., Keens, T. G., Wannamaker, E. M., Douglas, P. T., Crozier, N., Levison, H., and Aspin, N. Effects of gravity on tracheal mucus transport rates in normal subjects and in patients with cystic fibrosis. Pediatrics 50: 146–152 (1977).
117. Bateman, J. R., Pavia, D., and Clarke, S. W. The retention of lung secretions during the night in normal subjects. Clin. Sci. Mol. Med. 6: 523–527 (1978).
118. Pratt, S. A., Smith, M. H., Ladman, A. J., and Theodore, N. F. The ultrastructure of alveolar macrophages from human cigarette smokers and nonsmokers. Lab. Invest. 24: 331–338 (1971).
119. Leake, E. S., Gonzales-Ojeda, D., and Myrvik, Q. N. Enzymatic differences between normal alveolar macrophages and oil-induced peritoneal macrophages obtained from rabbits. Exptl. Cell Res. 33: 553 (1964).
120. Franson, R. C., and Waite, M. Lysosomal phospholipase A_1 and A_2 of normal and bacillus Calmette Guerin-induced alveolar macrophages. J. Cell Biol. 56: 621–627 (1973).
121. Brain, J. D. Macrophage damage in relation to the pathogenesis of lung diseases. Environ. Health Perspect. 35: 21–28 (1980).
122. Sanders, C. L. The distribution of inhaled plutonium-239 dioxide particles within pulmonary macrophages. Arch. Environ. Health 18: 904–912 (1969).
123. Brundelet, P. J. Experimental study of the dust clearance mechanism of the lung. Acta Pathol. Microbiol. Scand. 175: 1–141 (1965).
124. Green, G. M. Alveolobronchiolar transport mechanisms. Arch. Intern. Med. 131: 109–114 (1973).
125. Ferin, J. Lung clearance of particles. In: Air Pollution and the Lung (E. F. Aharonson, A. Ben-David and M. A. Klingberg, Eds.), Halsted Press-John Wiley, Jerusalem, 1976, pp. 64–78.
126. LaFuma, J., Masse, R., Metivier, H., Nolibe, D., Fritsch, P., Nenot, J. C., and Morin, M. Study of inhaled radio-active pollutants. In: Colloquium on Broncho-Pulmonary Reactions to Airborne Pollutants. Pont-a-Mousson, France, 1974.
127. LaFuma, J., Nenot, J. C., Morin, M., Masse, R., Metivier, H., Nolibe, D., and Skupinski, W. C. Experimental study on the toxicity of several radionuclides inhaled at different doses. In: Proceedings of the European IRPA Congress, CONF-750518-11, Amsterdam, Netherlands, 1975.
128. Stuart, B. O., Bair, W. J., and Park, J. F. Interpretation of excretion data from beagle dogs after ^{239}Pu inhalation. In: Diagnosis and Treatment of Deposited Radionuclides (H. A. Kornberg and W. D. Norwood, Eds.), Excerpta Medica Foundation, Amsterdam, 1968.
129. Phalen, R. F., Kenoyer, J. L., Crocker, T. T., and McClure, T. R. Effects of sulfate aerosols in combination with ozone on elimination of tracer particles by rats. J. Toxicol. Environ. Health 6: 797–810 (1980).
130. Brain, D. D. Free cells in the lungs – some aspects of their role, quantitation and regulation. Arch. Intern. Med. 126: 477–487 (1970).
131. Brain, J. D., and Corkery, G. C. The effect of increased particles on the endocytosis of radiocolloids by pulmonary macrophages in vivo: competitive and toxic effects. In: Inhaled Particles, Vol. IV, Part 2 (W. H. Walton, Ed.), Pergamon Press, Oxford, 1977, pp. 551–564.
132. Strecker, F. J. Tissue reactions in rat lungs after dust inhalation with special regard to the penetration of dust into the lung lymphatics and lymphatic nodes. In: Inhaled Particles and Vapours, Vol. II (C. N. Davies, Ed.), Pergamon Press, London, 1966.
133. Sorokin, S. P., and Brain, J. D. Pathways of clearance in mouse lungs exposed to iron oxide aerosols. Anat. Rec. 181: 581–625 (1975).
134. Davis, J. M. G., Ottery, J., and LeRoux, A. The effect of quartz and other noncoal dusts in coalworkers' pneumoconiosis. Part II. Lung autopsy study. In: Inhaled Particles, Vol. IV (W. H. Walton, Ed.), Pergamon Press, Oxford, 1977, pp. 691–702.
135. Morgan, A., Holmes, A., and Talbot, R. J. The fate of inhaled asbestos fibers deposited in the rat lung: a quantitative approach. In: Pulmonary Macrophages and Epithelial Cells (C. L. Sanders, R. P. Schneider, G. E. Dagle, and H. A. Ragan, Eds.), National Technical Information Service, Springfield, VA, 1977, pp. 436–450.
136. Beck, E. G., Bruch, J., Friedrichs, K. H., Hilscher, W., and Pott, F. Fibrous silicates in animal experiments and cell-culture

in morphological cell and tissue reactions according to different physical chemical influences. In: Inhaled Particles, Vol. III (W. H. Walton, Ed.), Unwin Brothers. Ltd., Old Woking, Surrey, 1971, pp. 477–486.
137. Allison, A. C. Mechanisms of macrophage damage in relation to the pathogenesis of some lung diseases. In: Respiratory Defense Mechanisms, Part II (J. D. Brain, D. F. Proctor and L. M. Reid, Eds.), Marcel Dekker, New York, 1977, pp. 1075–1102.
138. Thomas, R. G. An interspecies model for retention of inhaled particles. In: Assessment of Airborne Particles (T. T. Mercer, P. E. Morrow and W. Stober, Eds.), Charles C Thomas, Springfield, IL, 1972, pp. 405–420.
139. Stuart, B. O., Dionne, P. J., and Bair, W. J. A dynamic simulation of the retention and translocation of inhaled plutonium oxide in beagle dogs. In: Proceedings 11th AEC Air Conference, Vol. 2 (M. W. First and J. M. Morgan, Eds.), (CONF-700816), NTIS, Springfield, VA, 1970, pp. 721–737.
140. Stuart, B. O., and Beasley, T. M. Non-equilibrium tissue distributions of uranium and thorium following inhalation of uranium ore by rats. In: Inhaled Particles and Vapours, Vol. II (C. N. Davies, Ed.), Pergamon Press, Oxford-New York, 1967, pp. 291–298.
141. Mercer, T. T. On the role of particle size in the dissolution of lung burdens. Health Phys. 13: 1211–1221 (1967).
142. Stuart, B. O. Inhalation Risks from Radioactive Contaminants. Technical Report Ser. No. 142. International Atomic Energy Agency, Vienna, 1973.
143. Newton, Q. J., and Latren, R. K. Distribution in the beagle dog of ^{106}Ru-Rh aerosols subjected to thermal degradation. In: Fission Product Inhalation Program Annual Report 1970–1971. LF-44. Lovelace Foundation, Albuquerque, New Mexico, 1971, pp. 81–84.
144. Stuart, B. O. Promethium oxide inhalation studies. In: Pacific Northwest Laboratory Annual Report for 1965 in the Biological Sciences, BNWL-280. Battelle-Northwest, Richland, WA, 1966.
145. Stuart, B. O., Casey, H. W., and Bair, W. J. Acute and chronic effects of inhaled $^{144}CeO_2$ in dogs. Health Phys. 10: 1203–1209 (1964).
146. Morrow, P. E. Models for the study of the particle retention and elimination in the lung. In: Inhalation Carcinogenesis (M. G. Hanna, P. Nettesheim and J. R. Gilbert, Eds.), CONF-691001. NTIS, Springfield, VA, 1970, pp. 103–122.
147. Griffen, H. E. Health Effects of Exposure to Diesel Exhaust (Report of the Health Effects Panel of the Diesel Impacts Study Committee) National Academy Press, Washington, DC, 1971.
148. Moss, O. R. Dissolution of Uranium and Vanadium from Aerodynamically Size-Separated Ore Particles in a Simulated Lung Fluid. UR-3490.1005, University of Rochester, New York, 1976.
149. Moss, O. R., and Kanapilly, G. M. Dissolution of inhaled aerosols. In: Generation of Aerosols (K. Willeke, Ed.), Ann Arbor Science Publishers, Ann Arbor, MI, 1980, pp. 105–124.
150. NCRP Report No 60. Physical, Chemical and Biological Properties of Radiocerium Relevant to Radiation Protection Guidelines. National Council on Radiation Protection and Measurements, Washington, DC, 1979.
151. Craig, D. K., Brain, J. D., Cuddihy, R. G., Kanapilly, G., Phalen, R. F., Stuart, B. O., and Swift, D. L. Implications of the dosimetric model for the respiratory system in limits for intakes of radionuclides by workers. In: Proceedings of the Fifth International Symposium on Inhaled Particles and Vapors (ICRP Publication 30) (W. H. Walton, Ed.), Cardiff, Wales, in press.
152. Wilkey, D. D., and Lee, P. S. Mucociliary clearance of deposited particles from the human lung: intra- and inter-subject reproductivity total and regional lung clearance, and model comparisons. Arch. Environ. Health 35: 294–303 (1980).
153. Albert, R. E., Lippmann, M., and Briscoe, W. The characteristics of bronchial clearance in humans and the effects of cigarette smoking. Arch. Environ. Health 18: 738–755 (1969).
154. Thomson, M. L., and Short, M. D. Mucociliary functions in health, chronic obstructive airway disease, and asbestosis. J. Appl. Physiol. 25: 535–539 (1969).
155. Bohning, D. E., Albert, R. E., Lippmann, M., and Foster, W. M. Tracheobronchial particle deposition and clearance—a study of the effects of cigarette smoking in monozygotic twins. Arch. Environ. Health 20: 457–462 (1975).
156. Stuart, B. O., Palmer, R. F., Filipy, R. E., Dagle, G. E., and McDonald, K. E. Respiratory tract carcinogenesis in large and small experimental animals following daily inhalation of radon daughters and uranium ore dust. In: Proceedings of the IVth Congress of the International Radiation Protection Association, Paris, 1977, pp. 427–435.
157. Hursh, J. B., and Mercer, T. T. Measurement of ^{212}Pb loss rate from human lungs. J. Appl. Physiol., 28: 268–274 (1970).